

Adaptive Low Emission Microturbine for Renewable Fuels

Tavis J. Werts, Richard Hack and Vincent G. McDonell

ICAT Grant 06-12

**University of California, Irvine
February, 2010
(rev Nov 2011, rev 2, 31 Jan 2012)**

Conducted under an Innovative Clean Air Technology grant from the California Air Resources Board of the California Environmental Protection Agency

The statements and conclusions in this report are those of the grantee and not necessarily those of the California Air Resources Board. The mention of commercial products, their source, or their use in connection with material reported herein is not to be construed as actual or implied endorsement of such products.

Acknowledgments

We thank Kelly Benson, Michael Hackenberg and Suraj Nair from Woodward Inc. for their knowledge, support and time in the development and testing of the variable geometry injectors and ion sensor system.

We also thank Mark Mitchell and Junhua Chen at Capstone Turbine for their guidance in development of the system.

The support of Marc McDannel and the Los Angeles County Sanitation Districts is also acknowledged.

Support from Sempra Energy Utilities is also appreciated.

This report was submitted under Innovative Clean Air Technologies grant number 06-12 from the California Air Resources Board.

Content

Figures	iv
Tables	v
Nomenclature	v
Abstract	1
1 Introduction	2
2 Innovative Technology	3
3 ICAT Project.....	9
3.1 Injector Design.....	10
3.2 Characterization of the ion signal	13
3.2.1 Atmospheric Combustor Tests	13
3.2.2 Capstone C60 Engine Testing.....	18
3.2.3 Correlation Development.....	27
3.3 Algorithm Integration.....	31
3.4 Field Test.....	31
4 Status of the Technology	36
5 References.....	37

Figures

Figure 1 - Block Diagram of Technology.....	3
Figure 2 - ACCS Injector for Capstone C60 MTG.....	4
Figure 3 - Correlation between NO and Engine Combustor CO ₂ * Chemiluminescence Signal.....	5
Figure 4 - Correlation Between CO and %DC of the Engine Combustion Chemiluminescence Emission.	6
Figure 5 - Improvement Demonstrated for NO _x and CO Emissions Compared to Baseline for Natural Gas Operation as Load Varies.	6
Figure 6 - Typical NO _x vs Analyzed Ion Sensor Output.	8
Figure 7 - Cross Section of C60 Combustor.	10
Figure 8 - Actuator linkage installed on atmospheric combustor.	11
Figure 9 - CFD modeling results showing the OH* concentration of the fore plane of the C60 combustor.	12
Figure 10 - Redesigned ACCS injector for the Capstone C60.	12
Figure 11 - C60 Atmospheric Combustor.....	13
Figure 12 - Ion Probe positioned inside atmospheric combustor.	14
Figure 13 - Raw signal from 3 probe lengths - 12.7mm, 28.6mm and 41.3mm from left to right.	14
Figure 14 - Raw ion signal with local equivalence ratio shown at top.	15
Figure 15 - Moving average and standard deviation of ion signal. Local equivalence ratios are displayed above.	16
Figure 16 - Frequency response of the ion signal.....	17
Figure 17 - Ion Signal as the equivalence ratio (shown at top) of upstream injector is varied.	18
Figure 18 - Capstone C60 with a single ACCS injector installed.	19
Figure 19 - Average Ion Signal vs. Turbine Exit Temperature.	20
Figure 20 - NO _x Emissions vs Mean Ion Signal.....	20
Figure 21 - CO vs %DC.	21
Figure 22 - NO _x vs Mean Ion Signal for Various Days.	22
Figure 23 - CO vs %DC for Various Days.....	22
Figure 24 - Mean Ion Signal and NO _x Emissions versus % CO ₂ in fuel stream.....	23
Figure 25 - NO _x vs Mean Ion Signal with varying CO ₂ content.....	24
Figure 26 - %DC and CO Emissions versus % CO ₂ in fuel stream.....	24
Figure 27 - CO vs %DC for Various % CO ₂ levels.	25
Figure 28 - Capstone C60 with full set of ACCS injectors and actuators installed.....	26
Figure 29 - Raw Ion Signal vs Time (sec) - Six Injectors.	26
Figure 30 - Damaged center assembly and outer tube of injector.	28
Figure 31 - Ion probe glowing due to actuator angle.....	29
Figure 32 - Ion Signal Variation.....	30
Figure 33 - Variation of Standard Deviation.	31
Figure 34 - Installation at Santa Margarita Water District Chiquita Water Reclamation Facility.	33
Figure 35 - General Layout of Plumbing to Incorporate Gas Flow Metering.	34
Figure 36 - Output and Efficiency 28 Oct to 18 Nov 2011.....	35
Figure 37 - Temperatures in November 2011.....	35

Tables

Table 1 - Initial Two Level Factorial Design with repeated centerpoint.	27
Table 2 - Revised Two Level Factorial Design with repeated centerpoint.	29
Table 3 - Field Emissions Levels.	36

Nomenclature and Glossary

ACCS	Active Combustion Control System
CCADS	Combustion Control and Diagnostic Sensor
CFD	Computational Fluid Dynamics
CO	Carbon Monoxide
CO ₂	Carbon Dioxide
CO ₂ *	Electronically excited state of CO ₂ that results in spontaneous light emission from reaction (i.e., chemiluminescence)
C60	Capstone Turbine Corporation 60kW MTG
Equivalence Ratio	Ratio of actual fuel/air to stoichiometric fuel/air. Less than 1 indicates fuel lean conditions.
FFT	Fast Fourier Transform
Flashback	Undesired reaction propagation into the fuel/air premixer
kW	Kilowatt
Stoichiometric	Fuel/air combustion condition that results in no excess air or fuel
%DC	Ratio of amount of power in the low frequency range of the power spectra to total power spectra.
LBO	Lean Blow off (condition where the fuel/air ratio is too low to sustain the reaction—the reaction “blows off” at this condition)
MTG	Microturbine Generator
MW	Megawatts
NETL	National Energy Technology Laboratory
NO	Nitric Oxide
NO _x	Oxides of Nitrogen (primarily NO and NO ₂)
OH*	Charged hydroxyl radical species
OEM	Original Equipment Manufacturer
TET	Turbine Exit Temperature set point in the Capstone engine control software

Abstract

The objective of this Innovative Clean Air Technology research project was to reduce and maintain low emissions and improve the efficiency and reliability of a microturbine generator (MTG) system designed to burn renewable fuels. Some renewable fuels, such as methane emissions from landfills, vary in composition and are, as a result, challenging to burn efficiently and cleanly. To accomplish this, an Active Combustion Control System (ACCS) with a novel feedback sensor was implemented on an MTG. The ACCS uses a sensor, control logic, and variable geometry injectors to provide control of combustor fuel/air ratio independent of generator load. Active control provides a method to achieve low emissions while compensating for variation in fuel composition in both new and retrofit installations by allowing the system to monitor the combustion process and adapt to systematic and environmental changes. Information about the state of the combustion is obtained via various sensors incorporated into the injector. Woodward Incorporated worked with UC Irvine on the design of the injectors, including the actuation, control, and sensor integration and also provided key sensor and data recording equipment for the project. Using this equipment and the “smart injectors”, data from the reaction were obtained in the form of both light emission and electrical current. These data were analyzed and correlations with CO and NO_x emissions levels were developed. Woodward provided key support relative to interpretation and analysis of the signals obtained. A transfer function between emissions, fuel valve position, and the sensor outputs was developed using systematically controlled fuel compositions as provided by the gas blending facility at UC Irvine. Relations between NO_x emissions and ion mean signals were demonstrated which were insensitive to CO₂ concentrations. In addition, analyses of the dynamic aspect of the signal were related to CO concentration. Ultimately, however, the transfer functions proved overly sensitive to ion-probe position to be robustly integrated into a full closed loop system. This was noted through repetition of the tests with different ion-probe build ups. As a result, while a control system was conceptually developed around the ion signal and the actuated injectors, it could not be fully implemented on the engine due to this transfer function variability. Despite this, the engine was deployed with the variable geometry injectors developed for the project at a waste water treatment facility to evaluate the integrity of the variable geometry injectors and actuators. This >3700 hour trial demonstrated the integrity of the injectors and actuators which is a significant accomplishment. Further, the impact of the injector geometry on pollutant emissions was demonstrated, indicating that the variable geometry injectors were successful in reducing emissions. As a result, once a suitable robust sensing strategy is identified (e.g., pressure transducers or optical methods) the control system can likely be implemented successfully for closed loop operation to minimize emissions in light of variation in ambient conditions, engine wear, and fuel composition.

1 Introduction

The opportunity for alternative fuels usage in California is extensive. The annual energy potential from the combustion of two non-fossil alternative fuel sources in California are estimated be about 230 MW for landfill gas and 140 MW for anaerobic digestion gas(e.g., from both wastewater and livestock operations).¹ Even greater potential exists for gasified biomass from agricultural or forest operations (it is estimated to be at least a factor of 10 greater than the landfill/anaerobic digestion opportunity²). The viability of gasified biomass is tied in part to the availability of economic gasification technology. If this were available, the technology could offer similar its low emission benefit while burning a renewable fuel of variable composition/quality. Finally, the opportunity for co-firing natural gas with alternative fuels may also be of interest. In this case, the technology can help to ensure emissions are minimized for any mixture of natural gas and alternative fuel without modification of the engine or the fuel injectors.

To provide a specific example of emissions benefit, the following analysis is limited to the 97 MW worth of wasted energy from landfill gas that is currently flared or vented. First, it is apparent that installation of microturbine generators (MTGs) at these sites would have a dramatic impact on greenhouse gas emissions from applications where the gas is currently vented (approximately 31 MW worth of landfill gas) or flared (66 MW). For example, in the case of venting, adding the MTG would offset some 175,000 cubic feet per hour of methane containing gas. One molecule of methane has a much stronger global warming potential over 100 years than a molecule of CO₂ (~25-50 times). As a result, converting this gas to power has a significant greenhouse gas emission benefit for both greenhouse gas and criteria pollutants. In the case where the gas is flared, the greenhouse gas emission is reduced, but no useful product (e.g., electricity) is generated, which means additional power generation from existing sources is needed. As a result, the actual installation of an MTG at these sites will have a strong emissions benefit.

However, the trade off between greenhouse gas emissions and pollutant emissions cannot be overlooked. Because of advances in combustion technology, the Capstone Turbine Corporation C60 MTG can potentially offer reduced greenhouse gas emissions and very low pollutant emissions. The technology that is the subject of the project will be even more effective in reducing pollutant emissions because of its ability to adapt to variations in the precise composition of the landfill gas. To demonstrate the effectiveness of the project's technology, MTGs with and without the technology were compared. MTGs sited at landfills with this new technology would reduce CO emissions by about a factor of four compared to the baseline option without the technology. Based on characterization of the C60 MTG as a function of load, fuel composition, and combustion airflow^{3,4} this would translate into a reduction of CO emissions of around 1,275 tons/year in California. NO_x levels would be comparable to, or slightly lower than the baseline technology. This benefit would be even greater if co-firing or gasified biomass opportunities were considered as well. Maximizing flexibility relative to fuel composition is a twofold benefit. First, fuel composition at a given fuel source site, especially landfills, can vary in methane content over time from 35 to 65%.⁵ The Active Combustion Control System (ACCS) will ensure pollutant emissions are minimized as the fuel composition changes occur. Second, fuel variability from site to site is substantial due to varying life of the fill. The ability to turn down load as the gas production wanes also indicates a

need to optimize performance over a range of loads (50-100% load would be a reasonable practical range). Minimizing pollutant emissions in the absence of an ACCS requires customization of MTGs, or any other power generation device, for each site. The ACCS provides a standardized solution to the complex variety of fuels burned and the introduction into the market of an economically viable MTG suitable for use in a number of applications.

This report describes the development of an adaptive low emissions MTG that can minimize pollutant emissions over a range of fuel compositions.

2 Innovative Technology

The technology developed in this project is an Active Combustion Control System (ACCS) with a novel feedback sensor implemented on a microturbine generator (MTG). The ACCS uses variable geometry injectors to provide control of combustor fuel/air ratio independent of generator load. A non-intrusive ion sensor monitors the combustion process inside the engine in real time to allow for closed loop control of combustor chemistry (i.e., NO_x , CO, and combustor stability) as ambient conditions, load, and fuel composition vary. The ACCS system has been successfully demonstrated on a commercial MTG in a laboratory environment.

The overall components associated with the technology are shown in Figure 1. In demonstrations of the concept, a Capstone C60 commercial MTG was adapted to incorporate the technology as operated on natural gas.

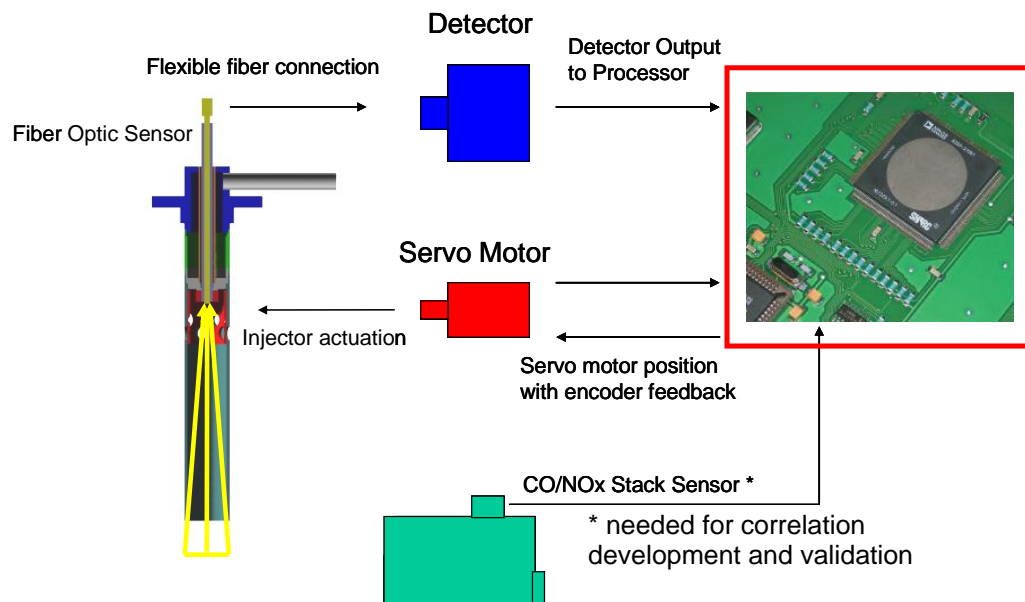


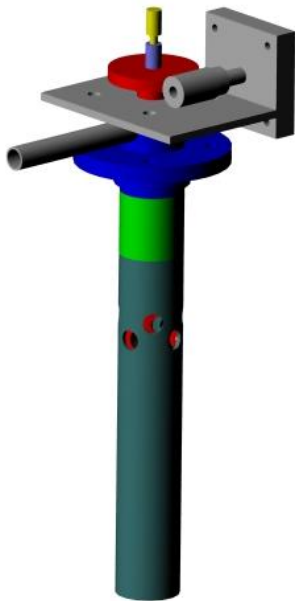
Figure 1 - Block Diagram of ACCS Technology.

The key components of the system include:

- Combustion sensor (device to monitor the combustion process and produce information regarding emissions either directly or indirectly)
- Controller (control system to instruct actuator based on information from the sensor)
- Actuator (device to modify the combustion process)

In the demonstrated system, the combustion sensor was based on light emission from the combustion chamber. This approach was adopted based on work in the literature that suggests specific relations between heat release and light emission.^{6,7} While the heat release relationship to light emission may seem intuitive, interpretation of the light emission and relating it to engine emissions of NO_x and CO is far less obvious. Nonetheless, such relations have been demonstrated previously and thus the light sensing approach appeared like a reasonable strategy.^{8,9} To allow in-situ monitoring of the light emission, a high temperature fiber optic was installed in the fuel injector which conveyed the light to a photomultiplier tube (PMT). The ACCS injector developed for the Capstone C60 MTG is shown in Figure 2. Note the location of the actuator and the use of silicon sealant (redish material) on the optical fiber passthrough. These strategies proved to be problematic as will be discussed below.

a) CAD Rendering of ACCS Injector



b) Injector Installed in C60 Combustor

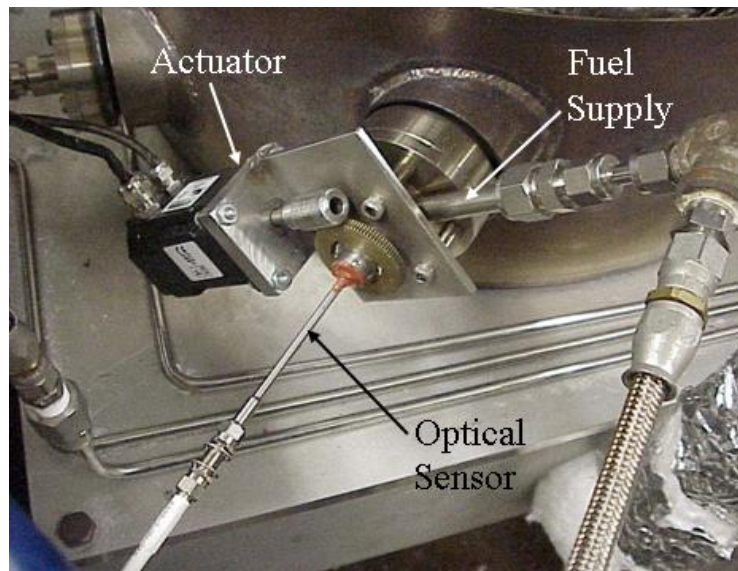


Figure 2 - ACCS Injector for Capstone C60 MTG.

The voltage signal produced by the PMT was interpreted by the controller by using algorithms developed which related the signals to NO_x and CO engine emissions. As a demonstration of proof of concept, NO_x was observed to be related to the general intensity of the light. The physical interpretation of this is associated with the well known relationship between NO_x and temperature. The light emission from the combustion

process is related to the temperature of the reaction; hence light emission and NO_x have a logical relationship to each other. Previous work has suggested that CO and combustion stability are associated with the dynamic behavior of the system.^{10,11} Intermittent light emission has been correlated with CO as large variations in CO occur when it is prevented from oxidizing to CO₂ (i.e., it's reaction is "quenched") in times when the combustion process is momentarily interrupted.

Figure 3 and Figure 4 illustrate the typical correlation between the sensor output and the engine exhaust emissions operated on natural gas for a range of loads. The NO emissions are related directly to the level of light intensity as shown in Figure 3. In this particular case, only NO was measured (as opposed to NO_x), but the majority of the NO_x emissions from gas turbines are associated with NO. This is consistent with the expected relation between light intensity and temperature⁷ which is directly correlated with NO formation rate. The CO emissions (Figure 4) are a function of the parameter "%DC" which is a parameter based on analysis of the light intensity signals. The %DC measurement is found by transforming the dynamic signal into the frequency domain via a fast Fourier transform (FFT) and summing the intensity of the signal at various frequencies. The portion of the signal at, or very near, 0 Hz can be said to be direct current, while the rest of the signal can be considered alternating current. The intensity of the 0 Hz "bin" (actually the intensity within the first bin, the width of which is a function of the sampling frequency and the discretization level of the FFT) divided by the total intensity of the signal give the %DC measurement. Conceptually, lower levels of %DC are associated with a more intermittent reaction which might be representative of a combustion system that is approaching a blow off limit. Higher levels of %DC reflect steady, stable combustion.

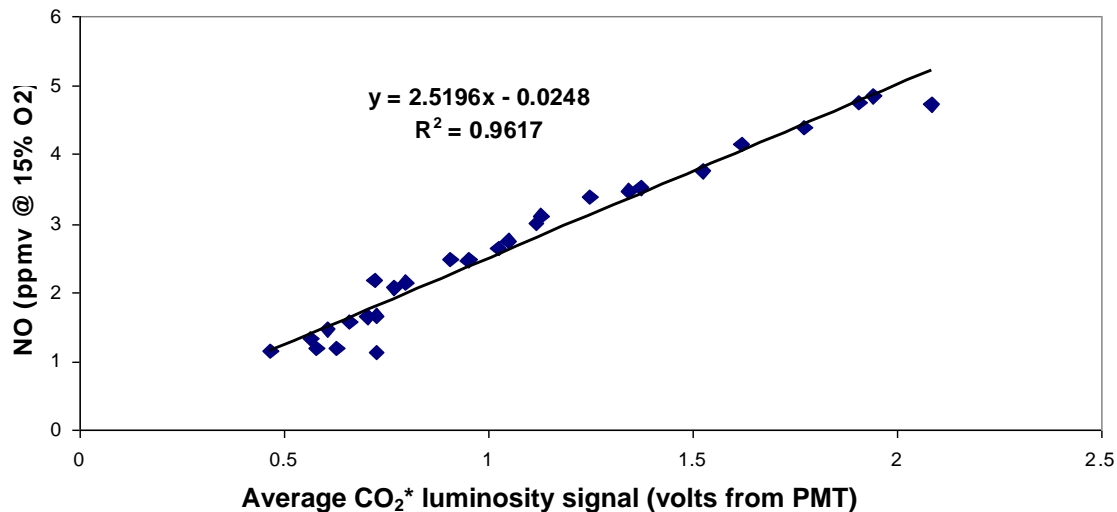


Figure 3 - Correlation between NO and Engine Combustor CO₂* Chemiluminescence Signal.

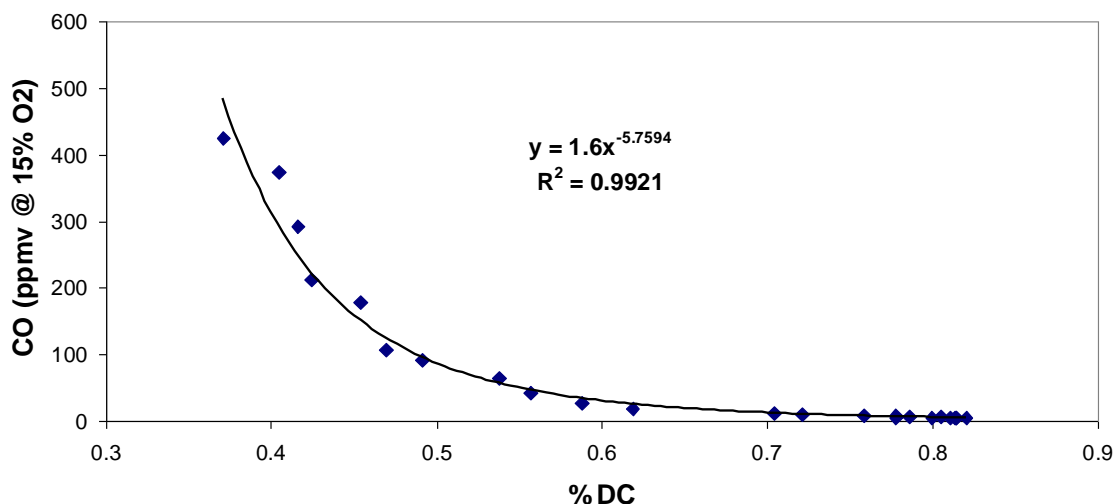


Figure 4 - Correlation Between CO and %DC of the Engine Combustion Chemiluminescence Emission.

The proof of concept system was demonstrated for operation on natural gas for a range of loads and was effective in significantly reducing CO emissions while maintaining or minimizing emissions of NO_x. Typical effectiveness is illustrated in Figure 5, relative to the performance of the current commercial MTG system. Results shown represent 5 minute averages after signals reached steady state following a change in the system operation. As shown, CO emissions are reduced from over 200 ppm to less than 50 ppm on average while NO_x emissions are also reduced by 10-25%. Unlike the example shown in Figure 3, NO_x was measured and reported in Figure 5.

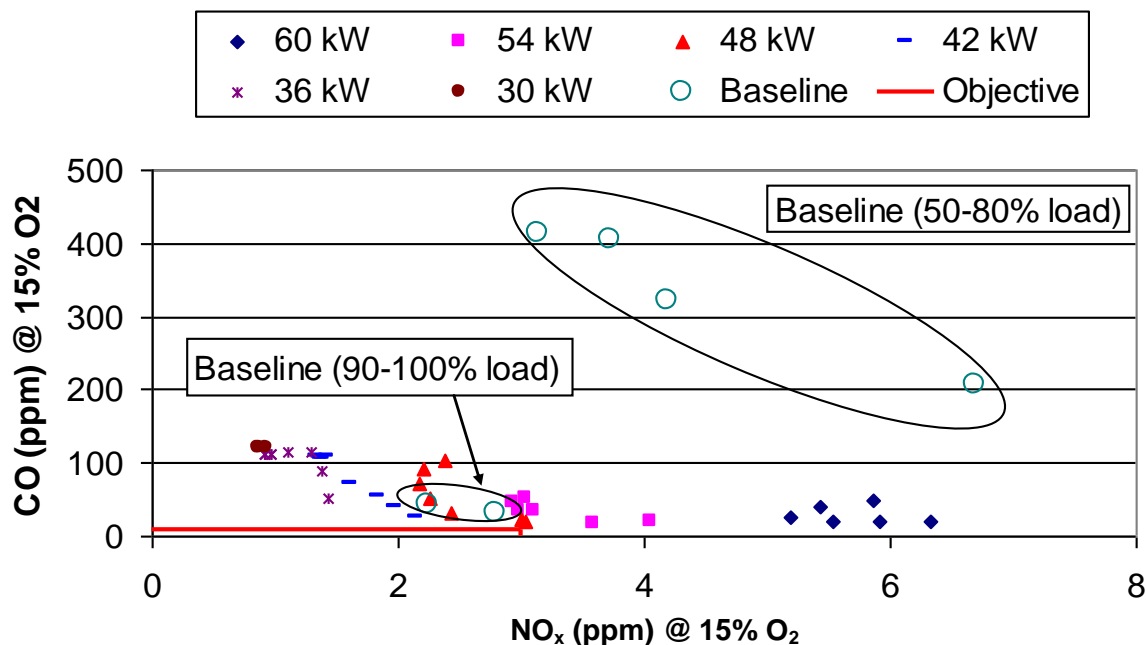


Figure 5 - Improvement Demonstrated for NO_x and CO Emissions Compared to Baseline for Natural Gas Operation as Load Varies.

Although successful, the proof of concept did present some critical shortcomings that need to be addressed, which is where the current project essentially starts. These key shortcomings are as follows:

1. The modifications made to the injectors relative to the axial position of the air holes resulted in some unexpected fuel/air mixing differences relative to the original equipment manufacturer (OEM) injectors.
2. Thermal stress on the actuator motor due to its proximity to the combustor liner was noted and essentially resulted in failure of the actuator within a few hours.
3. The seals developed for the prototype injector shown in Figure 2 leaked.
4. Only limited durability testing was carried out initially and was one of the primary objectives of the current effort. A key concern is associated with potential optical degradation of the fiber reducing the emissions signal over time.
5. The overall cost of a sensing system based on light emission was higher than desired.

To help overcome these limitations, Woodward, Incorporated was engaged on the project team. With their extensive experience in gas turbine component development and control systems, the shortcomings above could be best addressed. In terms of cost, the Woodward ion sensing technology as an alternative to the light sensing approach used previously (and which required relatively expensive optical component and detectors) is a key strategy. Woodward's ion sensing technology has been demonstrated on a number of gas turbine systems specifically for the detection of incipient blow off and thermoacoustic instabilities (i.e., combustion oscillations).

The shift to ion sensing was a significant change in the sensing strategy. The optical sensing approach relies upon excited molecules in the combustion region emitting photons. The ion sensing approach relies upon detection of charged particles in the combustion region. Woodward has successfully demonstrated ion sensing for flashback (the unwanted propagation of the reaction into the fuel/air premixer) and blow off sensing, but its use for emissions correlation had not been fully assessed. The presence of ions and excited molecules (used in the light sensing approach) are both naturally occurring phenomena in the combustion process. As a result, it seemed reasonable to expect that similar signal interpretation can be used to extend the ion sensing method to the inference of emissions. Hence, while ion sensing has not been specifically targeted as an emissions inference strategy, evaluation of existing datasets obtained on gas turbine combustion test rigs at National Energy Technology Laboratory (NETL) has demonstrated that correlations between ion sensing signals and NO_x can be developed as illustrated in Figure 6.¹² In this case, higher NO_x levels are associated with lower levels of %DC while incipient lean blow off (LBO) was found at higher levels of %DC. Intuitively, one might expect the opposite trend as higher %DC levels suggest "steadier" combustion. It is evident from this limited study that non-linearity in the response and seemingly multi-valued responses at low levels of %DC that additional work is needed to verify this strategy. Further, the generality of this trend and applicability to the Capstone engine and injector configuration had yet to be examined. Regardless, the relationship shown provides a starting point of a basis for correlating the NO_x emissions with the ion signal.

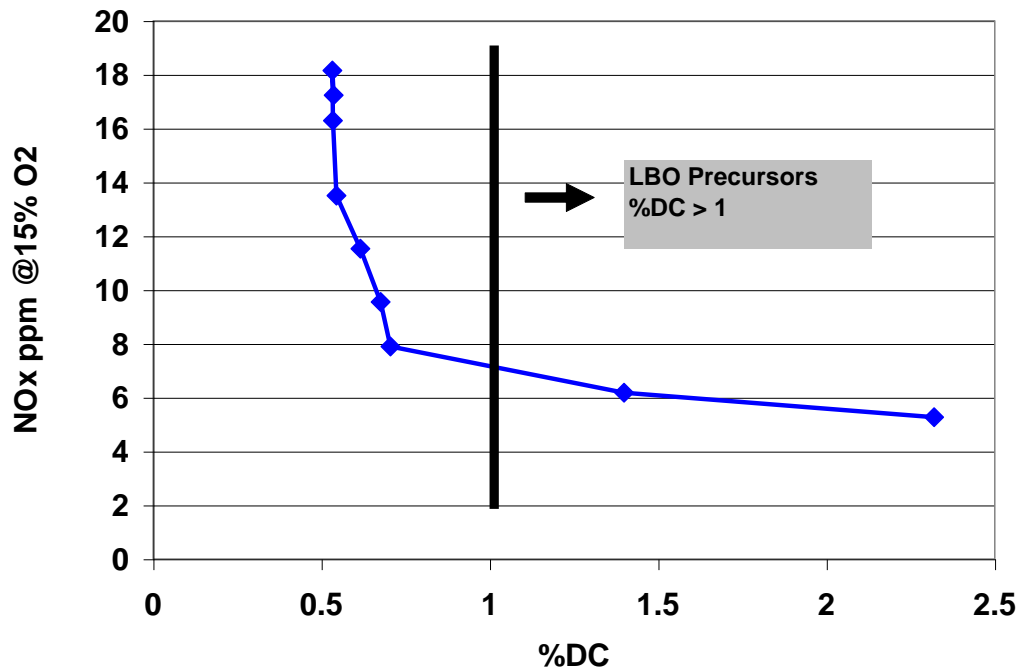


Figure 6 - Typical NO_x vs Analyzed Ion Sensor Output.¹²

As a result, it was decided to adopt this approach and explore its limits and application to (1) a different engine and (2) a different response (in this case, emissions). The use of the ion sensing technology was of direct interest to Woodward and thus helped to justify their participation in the program. The specific ion approach used in this project is based on Woodward's Combustion Control and Diagnostic Sensor (CCADS) technique. As suggested above, this system has been shown to be well-suited to detect combustion dynamics at gas turbine conditions¹³. Again, Woodward's overall experience in the provision of combustion fuel injection systems and control systems will also identify other strategies for cost reduction and elimination of the thermal stress issues previously observed.

The second innovative feature of the project is the extension of the system to alternative fuels (i.e., non-fossil fuels). A previous project conducted at UC Irvine on the Capstone C60 engine illustrated that CO emissions and engine stability was strongly influenced by the fuel composition. The key to controlling CO emissions while maintaining low NO_x emissions was altering the primary zone fuel/air ratio and expanding the operating range over which all injectors in the C60 are fired, which was accomplished by controlling the air flow admitted through the C60 injectors. The device developed under this project is capable of precisely doing this.

In summary, the innovation of this project is associated with development of a MTG that can operate on a fuel stream of varying composition while minimizing pollutant emissions produced over operating loads from 50 to 100%. This has not been demonstrated before and no commercial product that does this is available. The attractiveness of the system is that it "self monitors" its own operation, specifically regarding emissions. As a result, in addition to taking advantage of available alternative fuels to reduce overall CO₂ emissions, the new technology will assure minimization of

criteria pollutant emissions as well, even in light of variations in fuel composition and ambient conditions.

The project brings together technology developed for natural gas emissions minimization as a function of load with observations made for pollutant emissions when operating on alternative fuels. And it brings in a major gas turbine component and control system developer to complete the necessary steps to create a commercial product for the Capstone C60 MTG. The system was developed and then demonstrated at a waste water treatment facility and the ability to improve in emissions performance documented.

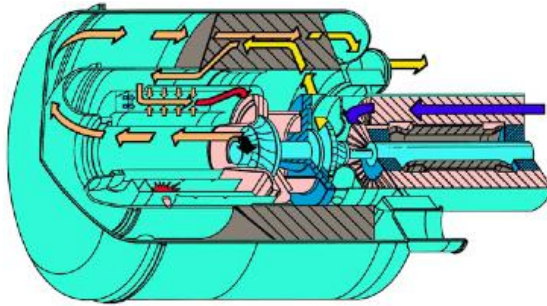
In terms of cost, the optical system demonstrated previously was estimated to increase the overall system cost by \$5,690 per MTG (about a 10% increase) based on instrumenting a single injector. This corresponds to about \$80-100 per kW. This cost is higher than desired. It would be desirable to add instrumentation to all injectors for a more robust system which would add an additional \$100 per kW. By incorporating the Woodward ion sensing technology and other technological developments, the cost of adding necessary sensors and actuation to the MTG system for all six injectors was reduced to \$50/kW. Additional refinements and production quantities could drive down costs even further.

Alternatives to accommodate the new technology are not commercially available for the MTG and are generally not cost-effective for small generation systems, which are ideally suited for the majority of the landfill/digester applications available. Selective catalytic reduction could be considered, but would add considerably more to the initial cost of the system as well as maintenance costs. Another factor relative to the use of a post-engine clean up approach is the variability in contaminants associated with the typical alternative fuels. As a result, unknown cost and durability questions relative to the applicability of these approaches to the MTG applications are issues. The new technology is adaptive to a wider range of fuel feedstocks and does not suffer from any limitations on temperature windows for successful operation. The technology is also completely retrofittable to all Capstone C60 engines, which increases the potential market availability in the near term.

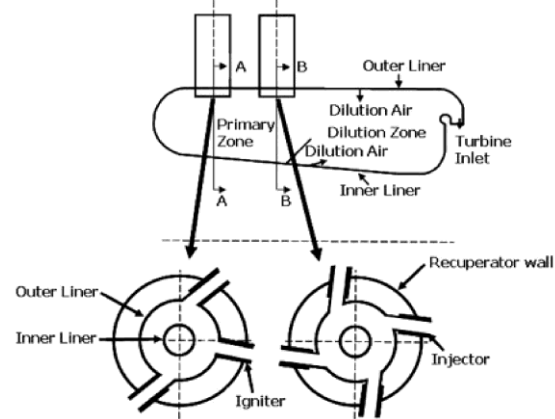
3 ICAT Project

The goal of this Innovative Clean Air Technology (ICAT) project was to incorporate active control features into the Capstone C60 microturbine generator and to use this technology to maintain ultra-low emissions as fuel composition varies. The C60 combustion system uses fuel staging to achieve very low emissions over a range of power output. Figure 7 illustrates the cross section of the combustor. As shown, the combustor has six fuel injectors located in two planes. The aft plane has two injectors, the fore plane has four injectors. Considerations relative to adding sensors to a single injector, multiple injectors, or other locations within the combustor were required. The overarching approach was to minimize modifications to the overall combustion system. As a result, retrofitting of one or more injectors was the desired implementation. As a result, the project essentially focused on injector modifications.

a) Capstone Gas Turbine Engine



b) Combustor Cross Section

**Figure 7 - Cross Section of C60 Combustor.**

3.1 Injector Design

The first step of the project was to redesign the injector with four goals in mind. First, the new injector must have a better sealing system in order to prevent air from leaking. Second, a new linkage system needed to be developed to move the actuator away from the engine in order to keep the temperature of the actuator within the operating regime. Third, the injector must incorporate the ion sensor probe in place of the fiber optic. Finally, durability issues needed to be anticipated and addressed in the design. Of particular concern is binding of the injectors' moving parts as well as maintaining sufficient positioning precision.

The sealing issue of the injectors was solved by Woodward using a high temperature O-ring seal at the variable geometry sleeve bearing surface. The tolerance was adjusted after initial testing to ensure that the variable geometry sleeve would not bind after sustained periods at operating temperature. Testing showed that there was no air leakage from the injector during operation at pressure.

Another serious shortcoming of the previously demonstrated injector was the thermal impact of the combustor on the actuator motor. With the actuators mounted directly to the injector body, heat from the injector body was transferred directly to the actuator, causing the magnets of the actuator to lose their magnetism. To rectify this, the actuator was moved away from the engine body by attaching an arm to the moving end of the injector. It was also connected, via a threaded rod and spherical rod ends, to a similar arm on the actuator (Figure 8). The actuator chosen was the Woodward L-Series actuator, which had favorable power requirements and range of motion. The distance between the engine and the actuators is adjustable based on the length of threaded rod chosen for the system.



Figure 8 - Actuator linkage installed on atmospheric combustor.

The CCADS system for this application works by applying a positive voltage potential to a probe running down the centerline of the injector. The body of the injector is grounded creating a voltage potential across a portion of the flame. Relative to incorporation of the ion sensor probe, several options were considered. A computational fluid dynamics (CFD) model of the combustor was used to help determine where the flame sits in the combustor. The concentration of the hydroxyl ion (OH^*) is useful for determining the location of the flame. As shown in Figure 9, there is a cone of unreacted fuel and air at the exit of the injector. One option considered was to put a bend in the ion probe in order to put the tip of the probe outside of the cone and into an area with a greater OH^* concentration. However this option was rejected for several reasons. First, concerns about the repeatability of a specific bend were raised. Due to the need for sealing and electrical isolation of the ion probe, the probe is thinner at the combustion end than the end outside the engine. This means that the probe must be inserted from the back end of the injector and that any bend made would have to be done once the probe was already installed into the injector. Ensuring that every probe was bent in the same location and to the same angle would have been prohibitively difficult. Second, concerns were raised that the bent probe could create a recirculation zone in the fuel/air flow and affect the position of the flame front within the combustor, possibly leading to a flashback issue. It was also decided that the bent probe would make installation of the injector into the engine extremely difficult. A tight tolerance between the injector and the engine body exists. Getting the injector installed without damaging or altering the positioning of the probe would be nearly impossible. Other shaped probes were considered, but rejected for the same reasons as the bent probe. Finally, it was decided that a straight probe would be the most reliable and easiest to install without affecting the flow within the engine. It was believed that if the probe were extended towards the tip of the reaction cone, the ion signal would be strong enough. Testing of this arrangement showed this to be true.

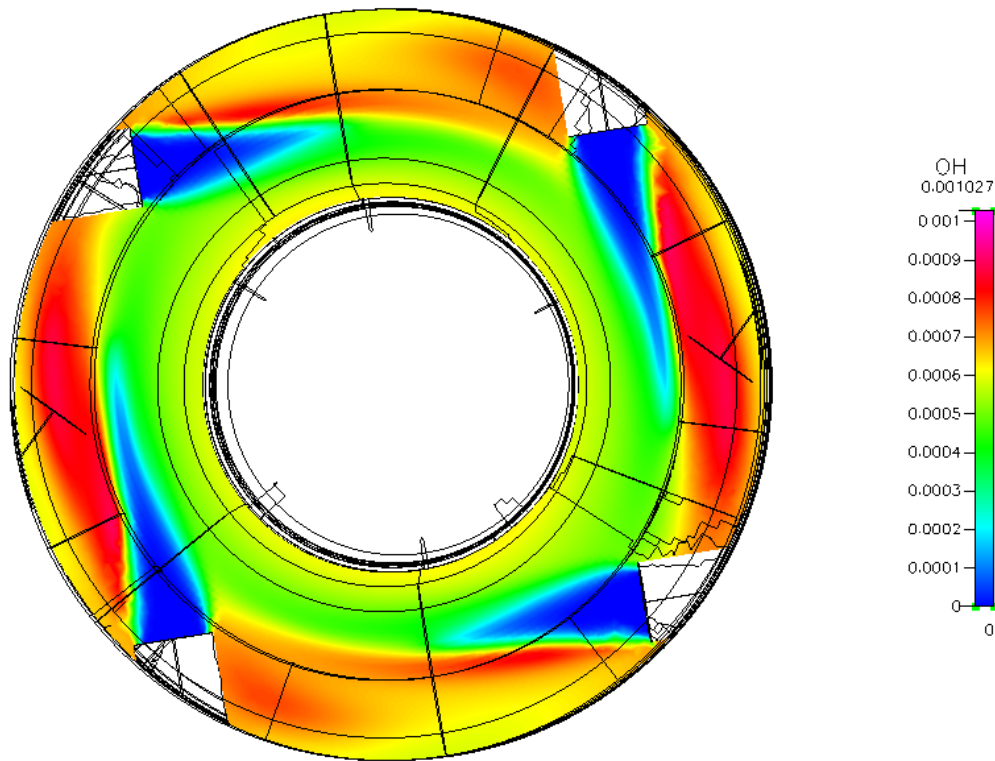
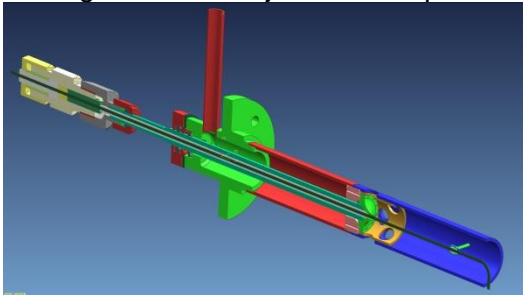


Figure 9 - CFD modeling results showing the OH* concentration of the fore plane of the C60 combustor.¹⁴

To incorporate the ion sensor probe, the fiber optic design was modified to accommodate the thinner ion probe. The ion probe is held in place and sealed using a Conex[®] fitting to ensure no air leaks past the probe. A ceramic tube runs down the center of the injector to isolate the ion probe from the injector body. The injector was designed so that, in addition to the ion probe, the fiber optic probe could be used in the event that more research with a fiber optic based system was desired. A drawing of an early “bent probe” concept and a photo of the final redesigned/fabricated injector are shown in Figure 10.

a) CAD Rendering of early redesigned ACCS Injector concept



b) Completed injector with ion probe and actuator arm

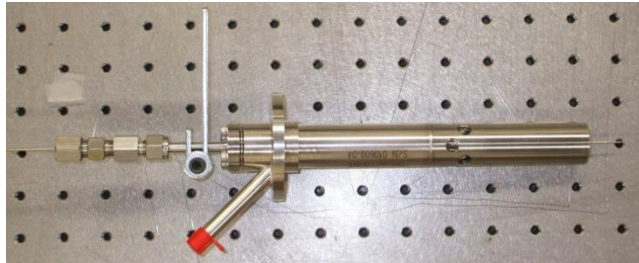


Figure 10 - Redesigned ACCS injector for the Capstone C60.

3.2 Characterization of the ion signal

Once the injector was designed and manufactured, the next step was to characterize how the ion signal would respond inside the combustor to varying flame properties. Initial testing was performed using an atmospheric combustor. Once confidence with the response of the probe and mechanical integrity was established, testing was moved to the actual engine.

3.2.1 Atmospheric Combustor Tests

The atmospheric combustor consists of the combustor section of a Capstone C60 turbine with all of the turbomachinery removed. This allows visual access to the combustor, as well as the ability to run the combustor under a large range of conditions without the concern of exceeding the material limitations of the turbomachinery. The air supply to the combustor is preheated and regulated to simulate the volumetric flow rate of the air flow in an actual C60 engine. Fuel is controlled independently for each of the injectors. The atmospheric combustor is shown in Figure 11.



Figure 11 - C60 Atmospheric Combustor.

A single ACCS injector was installed into the atmospheric combustor for initial stage of testing. Figure 12 shows the ACCS injector installed in the atmospheric combustor with the ion probe installed. First the engine was run with the ion probe to see what effect the probe might have on the position of the flame inside the combustor. Minimal effect on the flame front was seen. Next the position of the ion probe in respect to the flame front was investigated. Initial testing showed that the strength of the ion signal increased as the probe was moved further into the combustor. However, to increase the longevity of the probe it is desirable to position the probe in such a location as to keep the tip of the probe from glowing. Eventually a probe length of 28.6 mm beyond the exit plane of the

injector was chosen. At lengths beyond that, the tip of the ion probe would glow, especially when the actuator was partially closed, lowering the air velocity through the injector. This is discussed in more detail later.



Figure 12 - Ion Probe positioned inside atmospheric combustor.

The voltage potential (i.e., bias voltage) between the ion probe and injector body is adjustable with the Woodward hardware. This parameter was also studied in the atmospheric combustor. It was found that, as expected, a higher voltage potential lead to a stronger ion signal. The data acquisition hardware has an input voltage limit of 10 V, so the signal would saturate if the voltage were too high. It was found that, with a probe length of 28.6 mm, a bias voltage of 400V would provide a strong ion signal without saturating the data acquisition hardware (Figure 13).

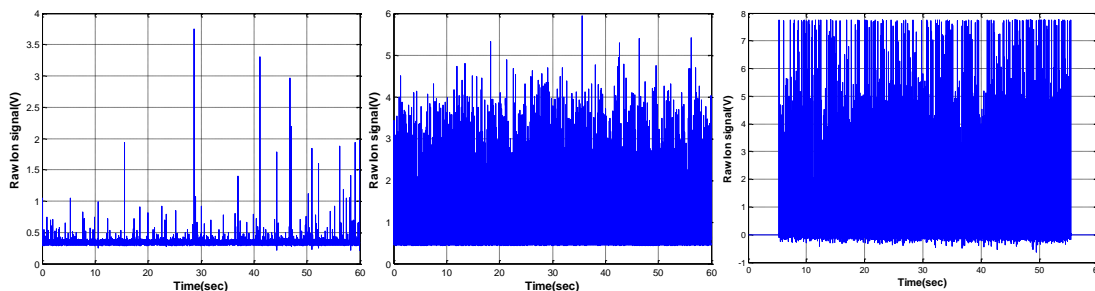


Figure 13 - Raw signal from 3 probe lengths - 12.7mm, 28.6mm and 41.3mm from left to right.

It is well established that NO_x emissions increase with temperature. It is also well established that, in the fuel lean combustion regime occurring in the C60 combustor, temperature increases with equivalence ratio. For a basic proof of concept, the ion

signal was recorded while the equivalence ratio of the injector was varied. The equivalence ratio is an indication of the amount of excess air present in the reaction, with values less than 1.0 indicating presence of excess air and greater than 1.0 indicating excess fuel. Current low emissions combustion systems tend to operate with a high amount of excess air (i.e., equivalence ratios below 1.0, down to 0.5-0.6) to help minimize combustion temperatures responsible for high NO formation rates.¹⁵ The raw signal from the ion sensor is shown in Figure 14. Although the signal is very dynamic, the overall amplitude of the signal increases with an increased equivalence ratio. This behavior is similar to the fiber optic signal from previous work.

To get a better feel for these trends, a 0.5 s moving average of the signal was calculated and plotted over the same time period. Those results are shown in Figure 15. Again the signal is shown to increase with equivalence ratio. Both plots show some discrepancy between the initial ignition equivalence ratio of 0.5 and the repeated 0.5 equivalence ratio at approximately 30 seconds, however the trend is evident. Also shown is the standard deviation of the ion signal. It follows the moving average trend quite closely.

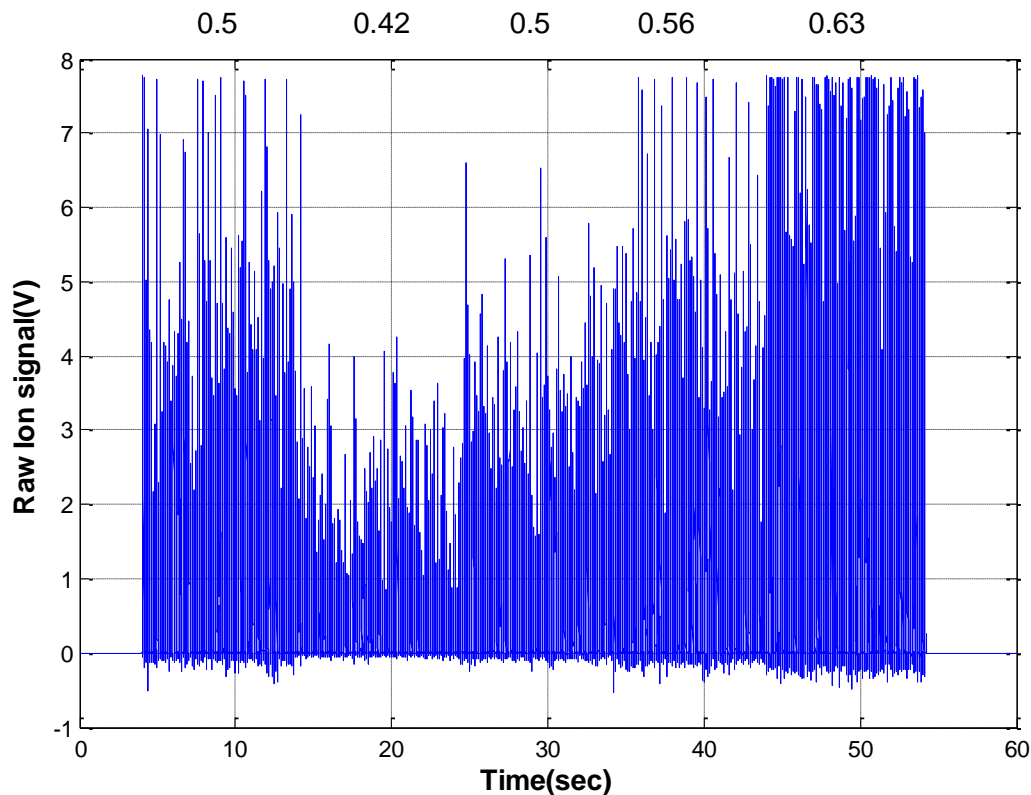


Figure 14 - Raw ion signal with local equivalence ratio shown at top.

The work with a fiber optic sensor showed a correlation between CO emissions and the dynamic %DC measurement of the signal. Knowing that CO emissions are also related to the temperature and, therefore, equivalence ratio of a reaction, a similar correlation was sought between the dynamic component of the ion signal and the equivalence ratio. The ion signal was transformed into the frequency domain and plotted over the same time period. As shown in Figure 16, at higher equivalence ratios, the intensity increases across all frequencies. Previous research by Woodward has shown that frequencies

above 3000 Hz are above the broadband combustion noise important for combustor control. For this reason a 3 kHz low pass filter was used to filter the ion signal.

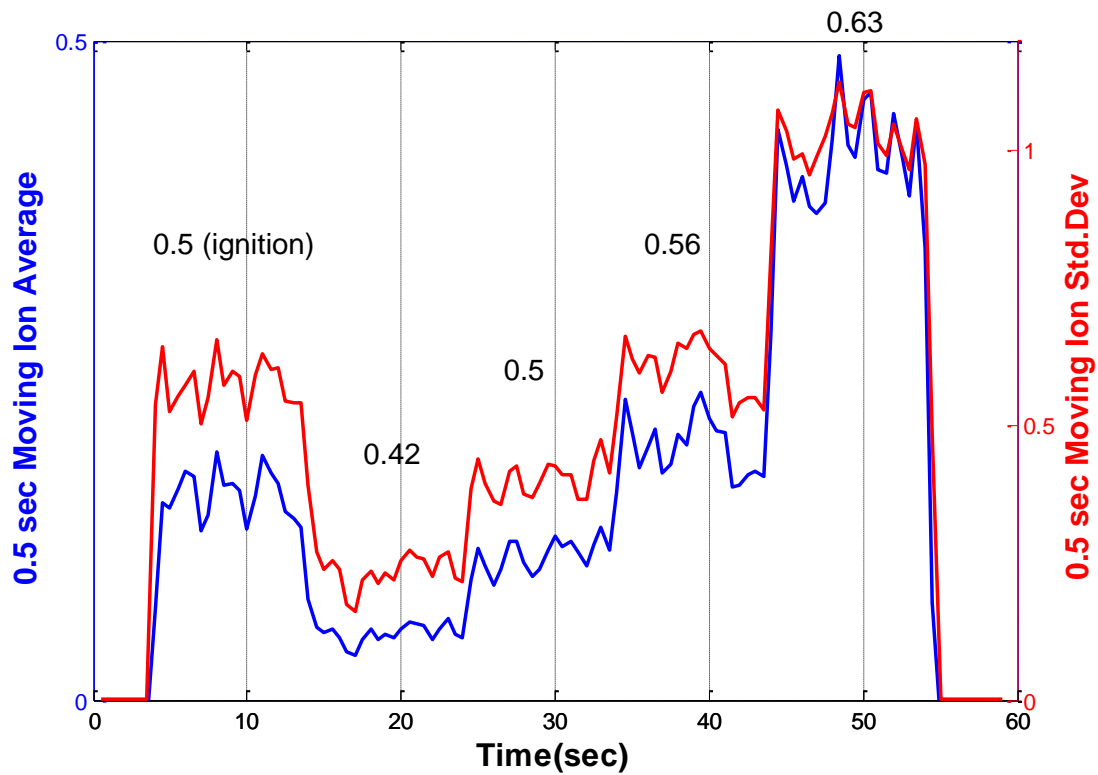


Figure 15 - Moving average and standard deviation of ion signal. Local equivalence ratios are displayed above.

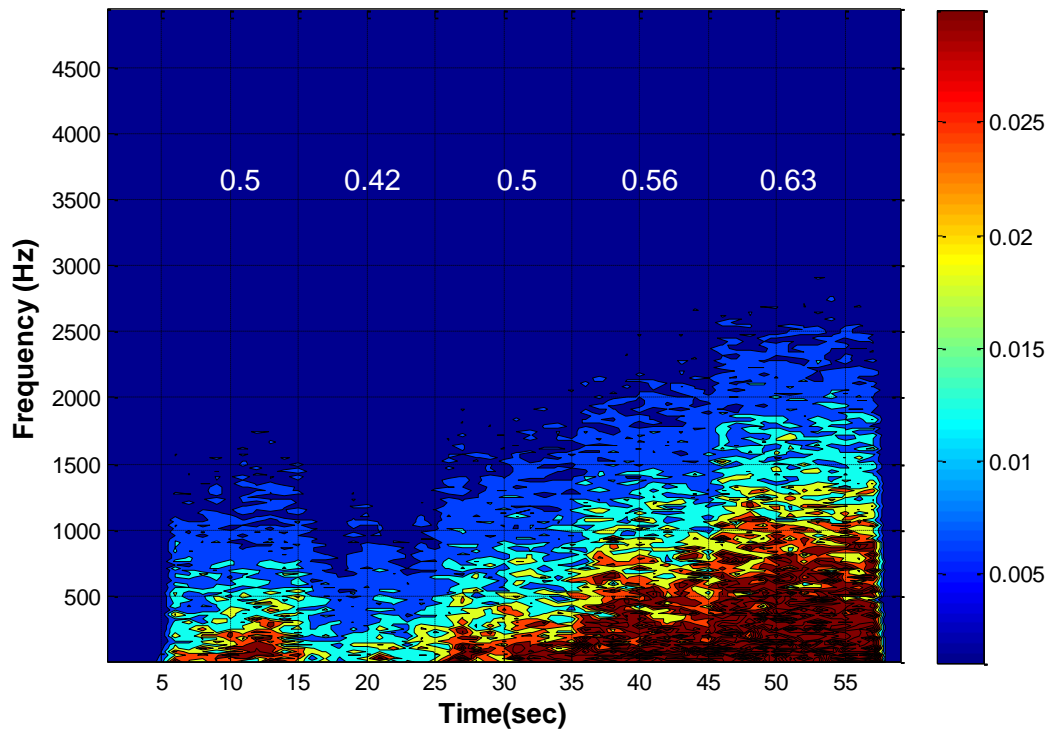


Figure 16 - Frequency response of the ion signal.

Further testing consisted of changing the equivalence ratio of the remaining five injectors while the ACCS injector was kept constant in order to investigate the effect that the other injectors had on the ion signal. Figure 17 shows the ion signal as the injector with the ion probe is kept constant while the equivalence ratio of the injector directly upstream is varied. No noticeable effect was seen, so it was concluded that the ion probe is negligibly affected by the upstream injectors.

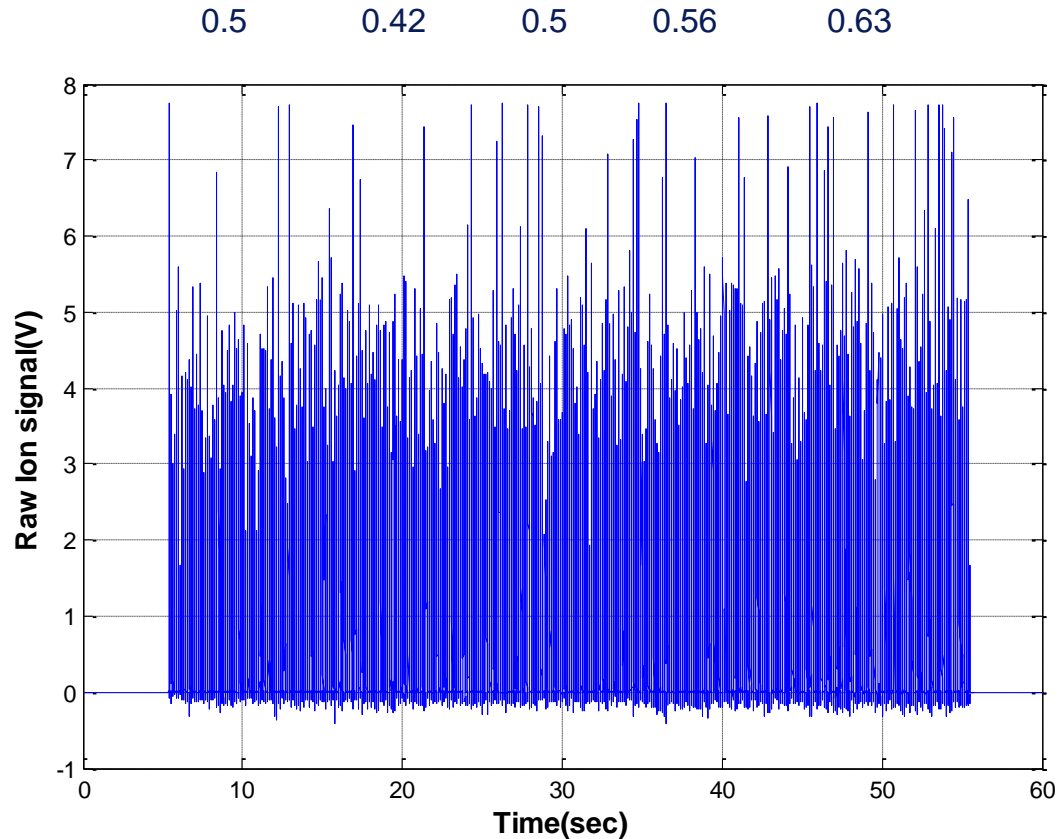


Figure 17 - Ion Signal as the equivalence ratio (shown at top) of upstream injector is varied.

3.2.2 Capstone C60 Engine Testing

With the proof of concept complete and a general understanding of the ion response to changes in equivalence ratio, the testing was moved to the Capstone C60 engine.

3.2.2.1 Single Injector Response—Natural Gas

In order to verify that the probe length of the atmospheric combustor was appropriate for the pressurized combustor of the engine, the ion probe was temporarily replaced with a thermocouple and the temperature was measured in 3 mm increments from the exit plane of the injector into the combustor. Results showed a temperature profile similar to the atmospheric combustor, and the probe length was kept at 28.6 mm. Initially a single ACCS injector was installed into the engine, shown in Figure 18. The first set of tests on the engine was similar to those performed in the atmospheric combustor. The equivalence ratio was varied and the ion signal recorded. Additionally, emissions data were recorded using a Horiba PG-250 emissions analyzer to build a direct correlation between the ion signal and the NO_x and CO emissions. The engine was controlled using the standard Capstone engine management software. The primary control signal for the stock engine is the turbine exit temperature (TET) which is a measurement of the temperature of the exhaust gas as it leaves the turbine section of the engine. At full load, the Capstone C60 normally runs with a TET set point of 635 °C which has been established by experience and is used for all fuel types. Changing it is not normally

done by the end user. By changing the TET set point of the engine management software, the engine will vary the fuel flow rate to achieve the desired TET, thus changing the equivalence ratio of the injectors. The TET cannot be set higher than that for fear of exceeding the material limitations of the turbine blades. When the TET set point is set below 600 °C, the engine becomes unstable. For this reason, the range of TET set points used was 600 to 635 °C. The TET set point was exploited to run the engine at a range of equivalence ratios to see the effect on both the ion signal and pollutant emissions. Since the engine control software makes changes more gradually than can be made in the atmospheric combustor, the ion signal was recorded for 60 second time periods with the engine running at steady state for the test. The ion signal was then averaged over that 60 second period for both the mean ion signal voltage, and the average %DC recorded during the testing period. Concurrently, the NO_x and CO emissions were noted during the same period. The 60 second period would represent sufficient time resolution for practical control bandwidth in the field. Attempting to respond to fuel composition changes faster than that would likely result in “overtuning” of the engine.

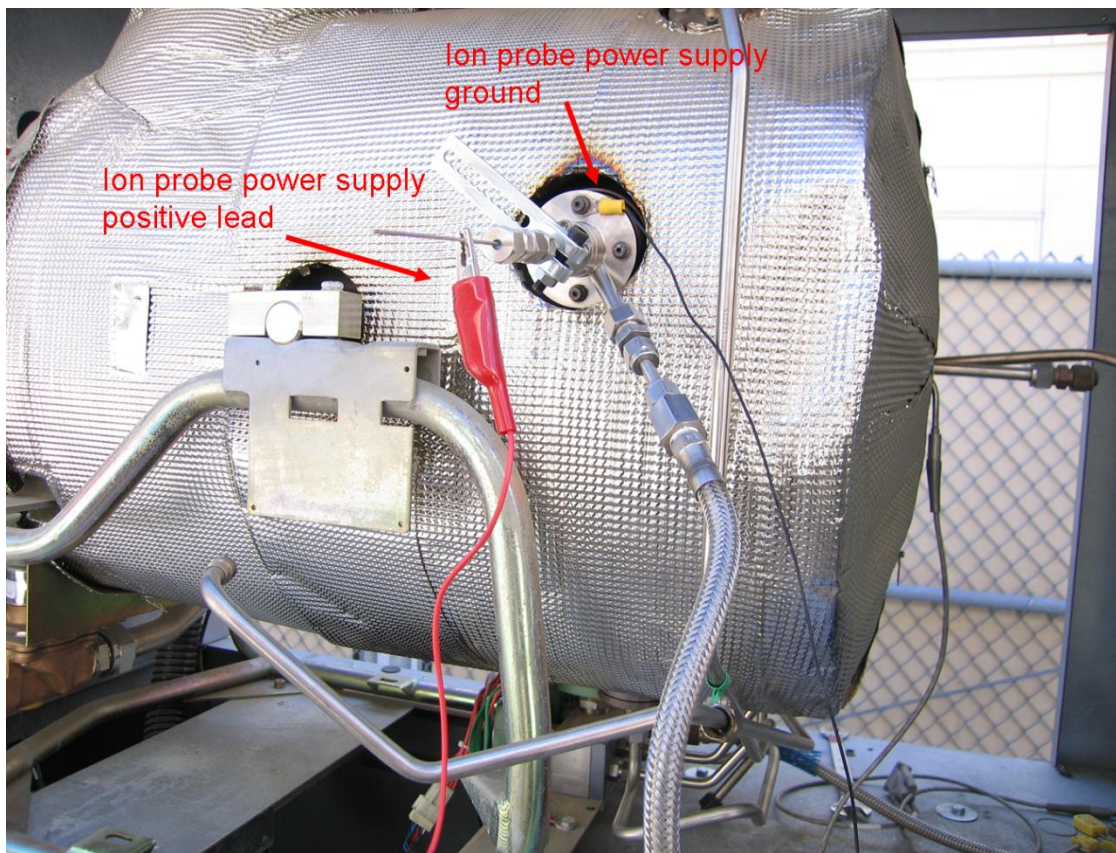


Figure 18 - Capstone C60 with a single ACCS injector installed.

When the mean ion signal is plotted versus temperature, an obvious trend is seen as the ion signal voltage increases with temperature (Figure 19). This was the expected result from the atmospheric combustor tests. The actual meaning of this trend is difficult to discern as the effect of the engine recuperator makes the increase in equivalence ratio nonlinear with an increase in TET. Instead, it is more useful to plot the average ion signal versus the NO_x emissions, as that is the parameter which is ultimately to be minimized. When shown versus the NO_x emissions (Figure 20), the mean ion signal

voltage increases linearly with NO_x . This is a key result that helps verify that the ion approach can indeed be used to infer NO_x emissions.

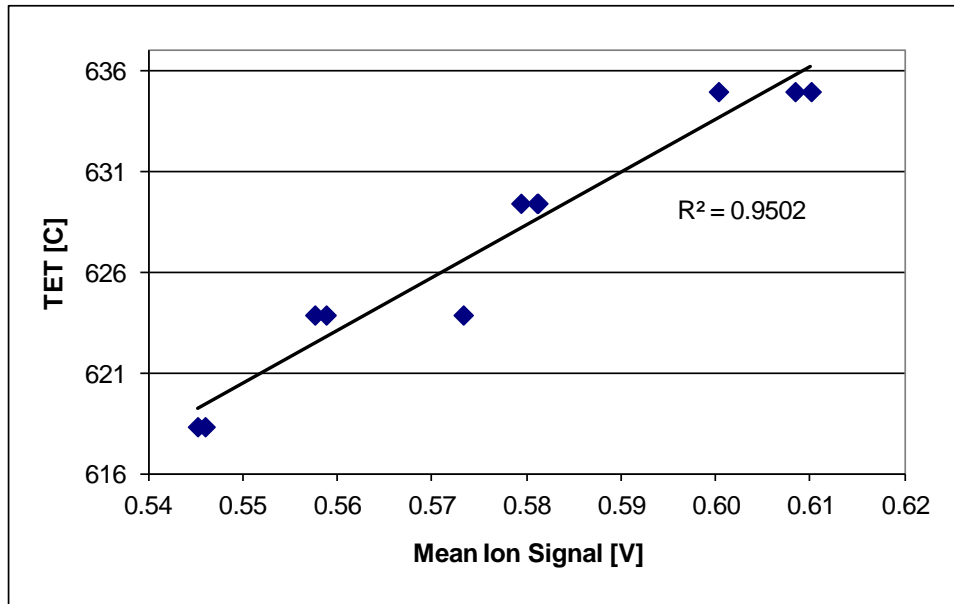


Figure 19 - Average Ion Signal vs. Turbine Exit Temperature.

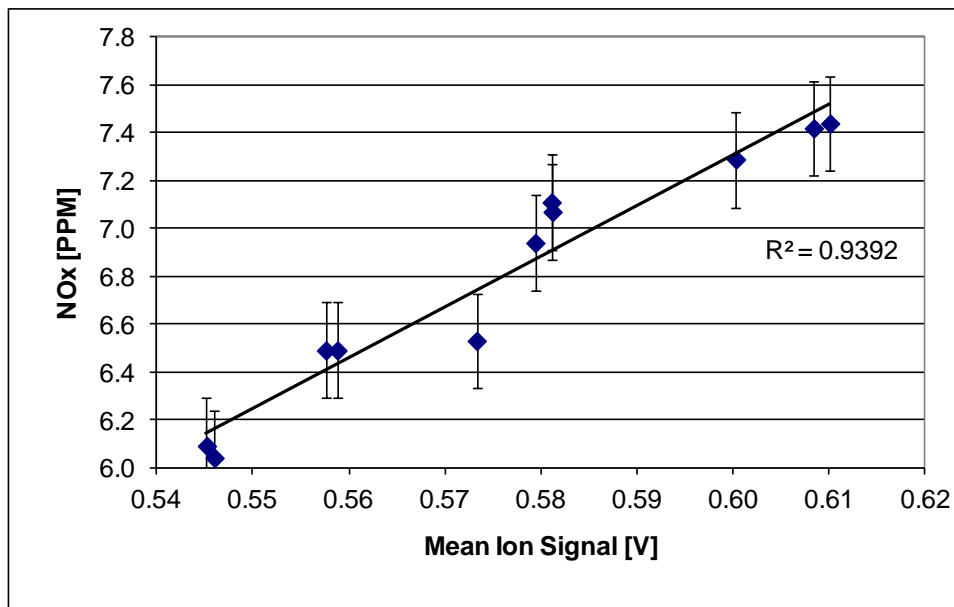


Figure 20 - NO_x Emissions vs Mean Ion Signal.

With the success attained relative to relating the ion signal amplitude to NO_x emissions, attention was directed to the CO emissions. Previously the %DC of the signal was found to correlate with CO for the light emission (recall Figure 4). As a result, this correlation was sought for the ion signal as well. The average %DC of the ion signal was calculated and plotted against CO emissions of the engine. Like the NO_x versus average ion signal voltage, a correlation is evident as shown in Figure 21. The overall levels of CO shown in Figure 21 are lower than those in Figure 4 because only small changes in load were examined in the current work at this point. The light emission based results show an

inverse relationship between the CO and %DC. In this case, like the results for NO_x demonstrated in early Woodward tests shown in Figure 6, the behavior of the CO and %DC contradict what would be expected. Higher levels of %DC indicate steadier combustion and generally CO will increase as combustion becomes less stable. This non-intuitive result eventually appeared to an anomaly as is discussed below. As a result, the otherwise promising results shown in Figure 20 and Figure 21 were fraught with inherent challenges as would be demonstrated in subsequent tests of repeatability of the results.

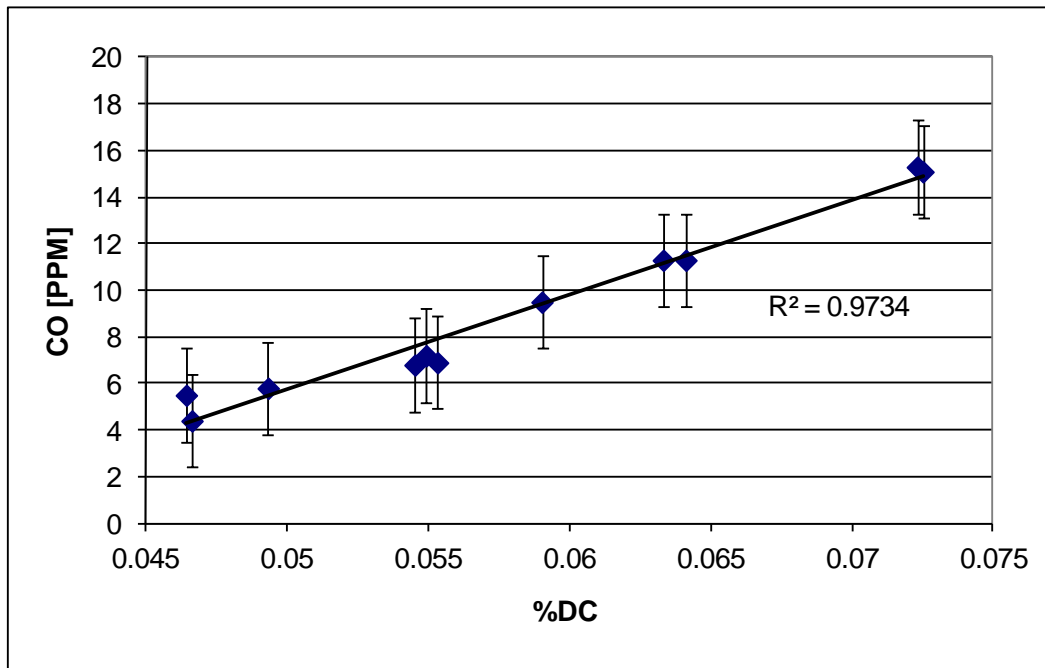


Figure 21 - CO vs %DC.

Subsequent tests obtained over various periods of time with fixed TET settings (as would be occur in practice) evaluated the robustness of the single injector results. These results were obtained by varying the load of the engine which has previously been shown to change NO_x (reduction as load decreases) and CO (increases as load decreases). A subtlety here is associated with the operation of the C60 engine. As mentioned relative to Figure 7, the C60 achieves low emissions for a range of loads by “staging” different numbers of injectors. Hence, it was important to consider conditions where all six injectors were actually fired (from approximately 52 to 60kW) otherwise additional variation would result. Given the consideration of full load with six injectors fired, examples of data obtained on various days are shown in Figure 22 and Figure 23. Figure 22 shows the NO_x levels vs mean ion signal for three different days. As shown, the general trend is similar to that shown in the original single injector engine test shown in Figure 20, but the slopes differ and variation is noted. Some of the variability is attributed to removal and reinsertion of the ion probe between the original tests (Figure 20) and the later tests shown in Figure 22. The results for CO are more troubling in one sense, but good in another. Troubling is the larger variation in the correlation between CO and %DC. The high variability is also evident. In this particular case, the variability compared to the original test shown in Figure 21 is much larger. The positive aspect of the results is that the trend observed in these tests makes sense—the more dynamic reaction (indicated by lower %DC values is associated with higher CO.

Regardless, the noted variability when examining day to day variation in the single injector tests poses a significant challenge relative to implementation of this approach in the current configuration. Essentially, it appears that the system is sensitive to factors that cannot be controlled precisely enough (e.g, exact location of the ion probe, ambient conditions)

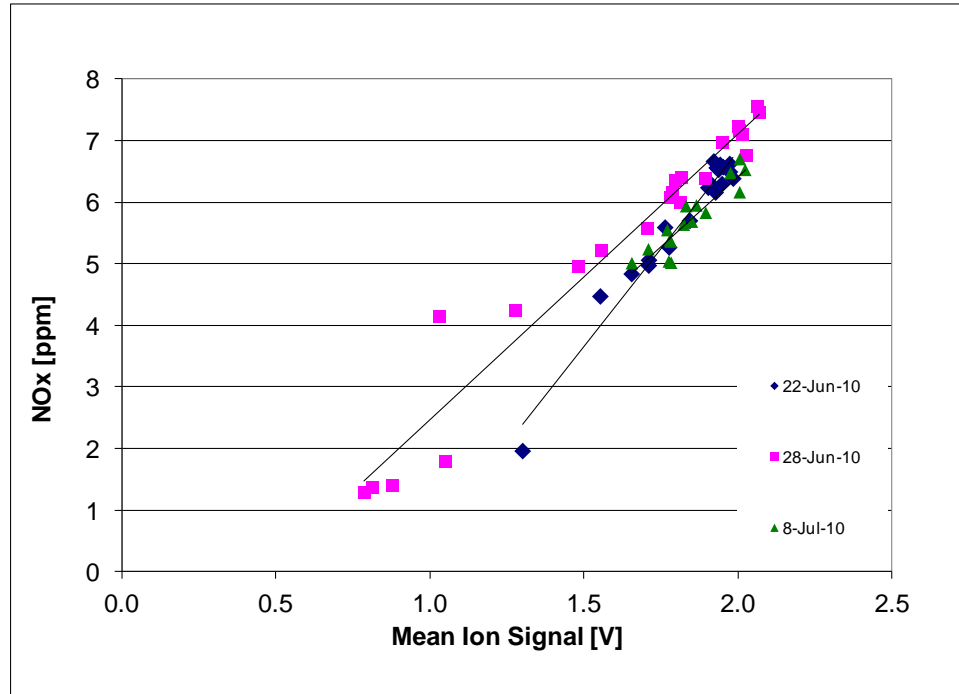


Figure 22 - NOx vs Mean Ion Signal for Various Days.

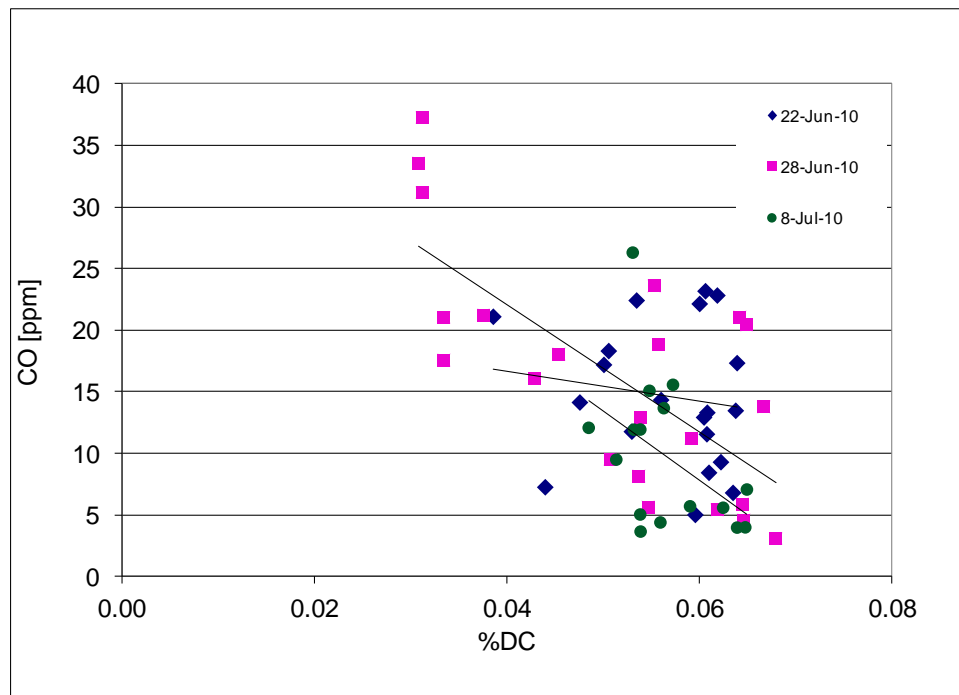


Figure 23 - CO vs %DC for Various Days.

Although variability is noted, a general trend for both NO_x and CO is noted and suggests the ion sensor has potential for correlation NO_x and CO results, although it is not nearly as robust as would be needed for the desired purpose. It is possible a more rigorous positioning of the sensor would help, but extensive discussions with Woodward established the centerline positioning used in this study. Despite the difficulty with robustness, it was decided to introducing fuel composition variation into the study to evaluate the response of the ion probe to diluents as would be encountered in waste water or landfill applications..

3.2.2.2 Response to CO_2 Content in Fuel

In order to simulate anaerobic digester and landfill gas, and investigate the effect of lower heating value fuel on the signal, the fuel stream was diluted with CO_2 . Using the on-site gas mixing station, the fuel supply can be diluted while the engine is running. For each set of test conditions, the fuel was diluted, and the testing performed after the system had returned to a steady state. Similar 60 second test runs were performed and the averaging procedure used above was applied to the signal was calculated to determine the mean signal level. It is evident from Figure 24 that the mean ion signal closely follows the trend of NO_x emissions even as the fuel is diluted. To reaffirm this, the NO_x is plotted vs the mean ion signal for the various CO_2 levels studied is shown in Figure 25. The linear correlation demonstrates that the ion signal is a reliable combustion control sensor of NO_x emissions for landfill gas since it is not affected by the diluent.

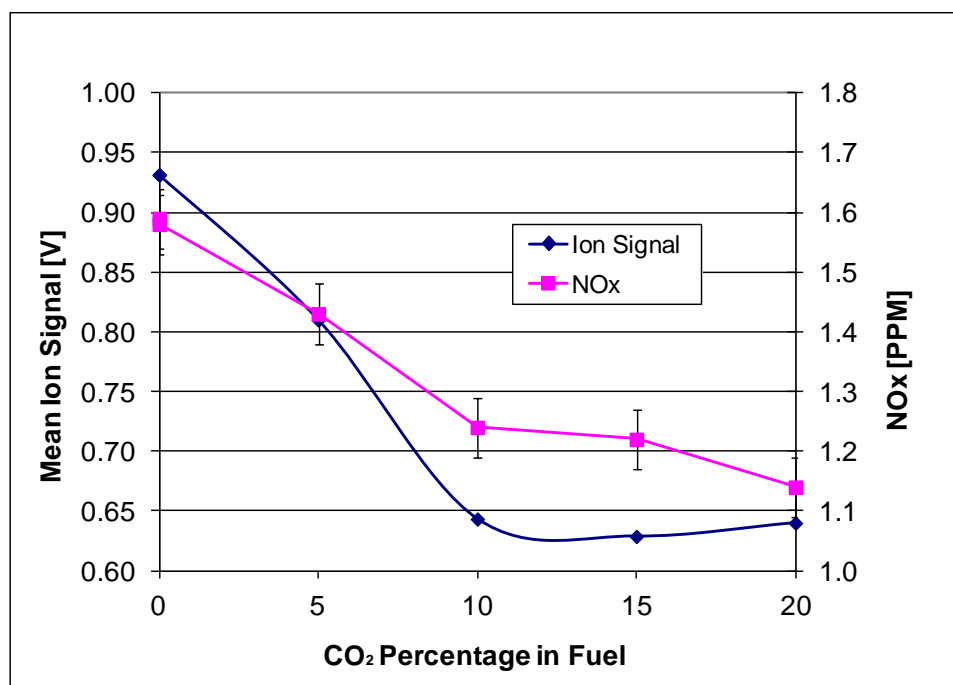


Figure 24 - Mean Ion Signal and NO_x Emissions versus % CO_2 in fuel stream.

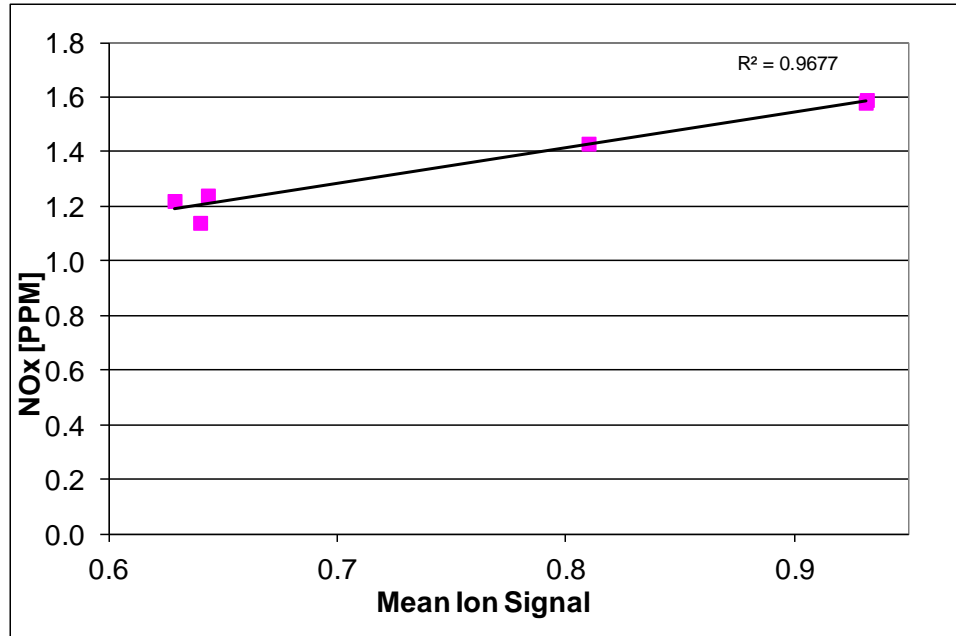


Figure 25 - NOx vs Mean Ion Signal with varying CO₂ content.

%DC and CO emissions versus % CO₂ in the fuel stream is shown in Figure 26. Figure 27 presents the information as CO versus %DC to help illustrate the correlation independent of CO₂ content. Note that this trend is opposite of that shown in Figure 21 but is consistent with the subsequent test done on various days shown in Figure 23.

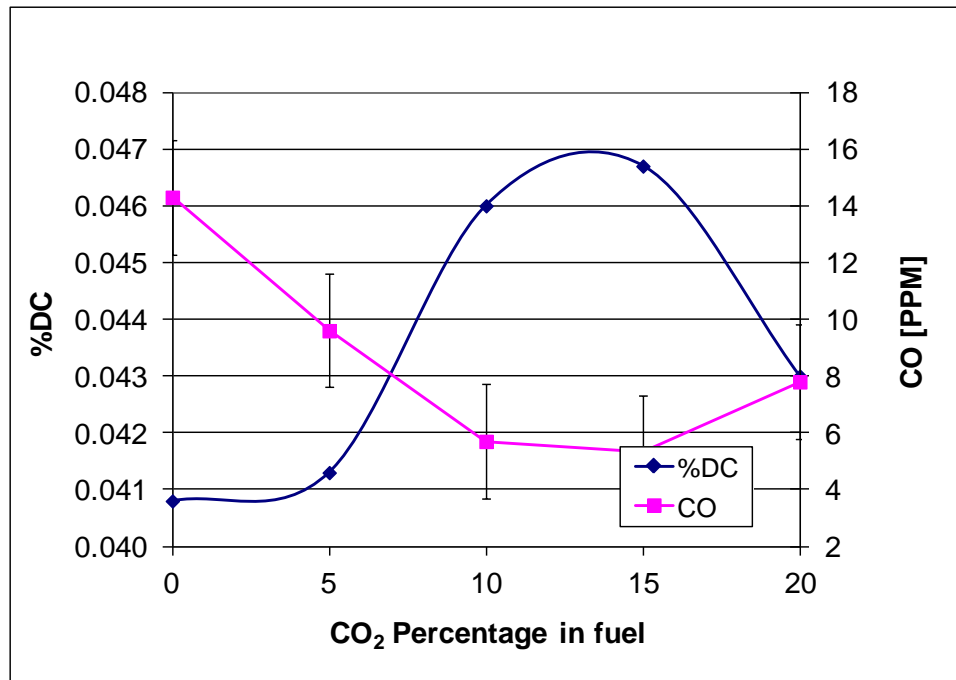


Figure 26 - %DC and CO Emissions versus % CO₂ in fuel stream.

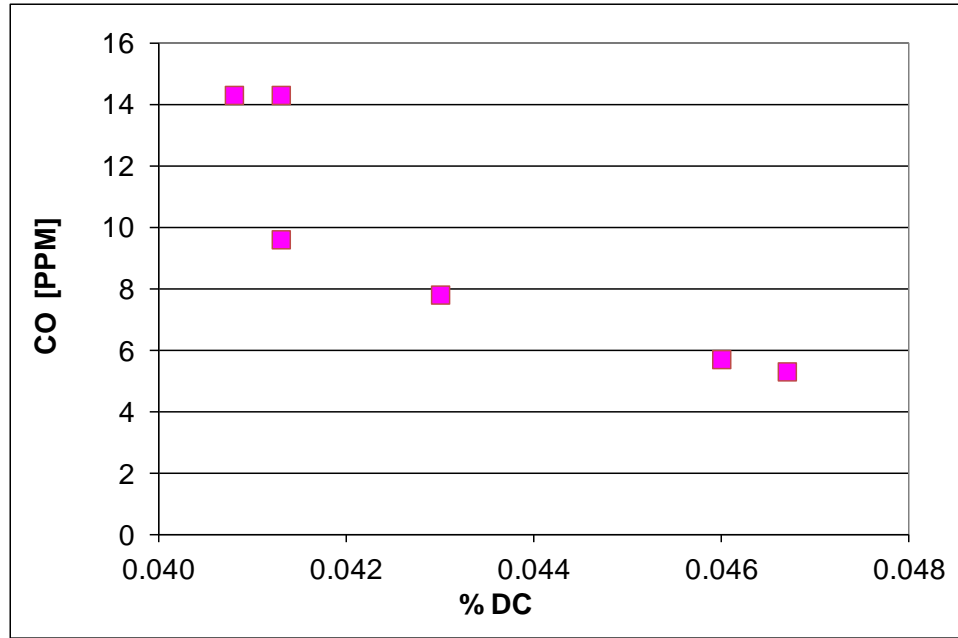


Figure 27 - CO vs %DC for Various %CO₂ levels.

The results suggest that the ion sensor response still tracks NO_x and CO emissions levels regardless of CO₂ addition. As a result, for the purpose of a control signal, it appears reasonable for the control algorithm to simply minimize the mean ion signal (i.e., reduce NO_x) and to maximize %DC (i.e., reduce CO). Hence it is not actually required to know the actual CO₂ level in the fuel. This is a significant finding relative to applicability of the ion signal for dilute fuels.

3.2.2.3 Multiple Injector Response Testing

The next step in testing was to install a full set of six injectors into the engine to examine the variation between signals from multiple injectors (Figure 28). Initial testing on the atmospheric combustor had shown that probe length can have a considerable effect on the intensity of the ion signal. It was also assumed that the aft plane of the combustor (recall Figure 7), which consists of two injectors, would have a weaker signal than the fore plane of injectors consisting of four injectors just downstream of the aft plane (again see Figure 7). Shown in Figure 29, there is noticeable variation between the injectors. “Ion 1” and “Ion 2” are the aft plane injectors and they have a lower amplitude signal than the injectors in the fore plane (“Ion 3” through “Ion 6”). The greatest variation is between injectors four and five, with injector five having an amplitude twice as strong as injector four. After this test was run the injectors were inspected and it was discovered that the difference in length was approximately 3 mm, with the probe in injector four being slightly less than the planned length of 28.6 mm, and the probe in injector five being about 1 mm longer than desired. This demonstrates that the tolerance on probe length is vital to the commercialization of the ACCS. This is also consistent with the observations in the day to day variation noted in the single injector studies reported in Section 3.2.2.1. Ideally, the transfer function between emissions and ion signal should be based on normalized results to reduce this sensitivity, however, it is anticipated that the variability from day to day may still impact the robustness of the correlation.

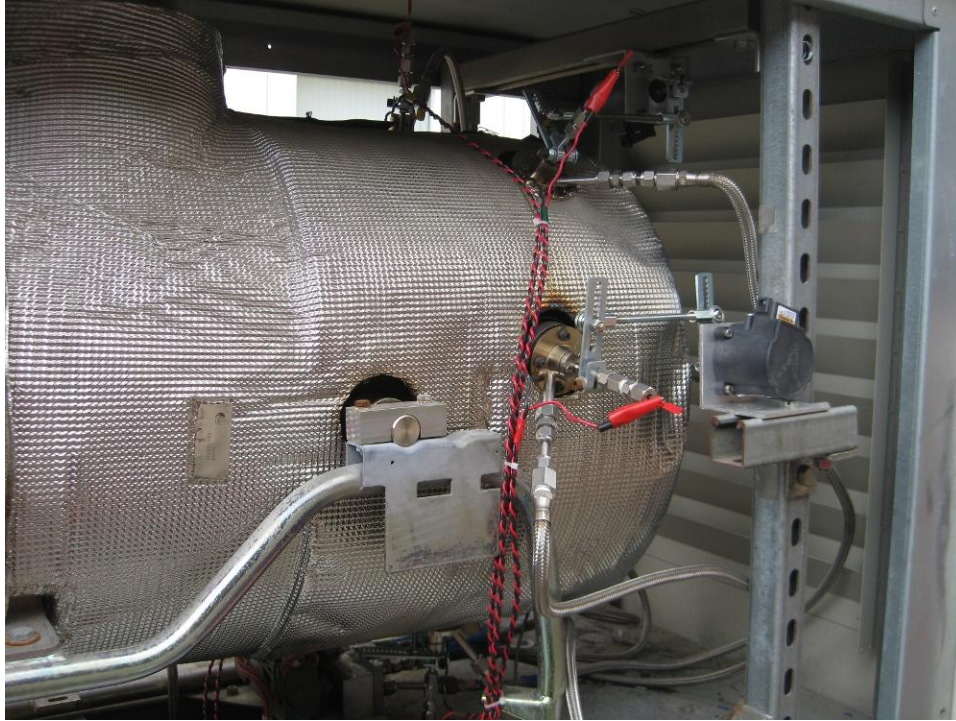


Figure 28 - Capstone C60 with full set of ACCS injectors and actuators installed.

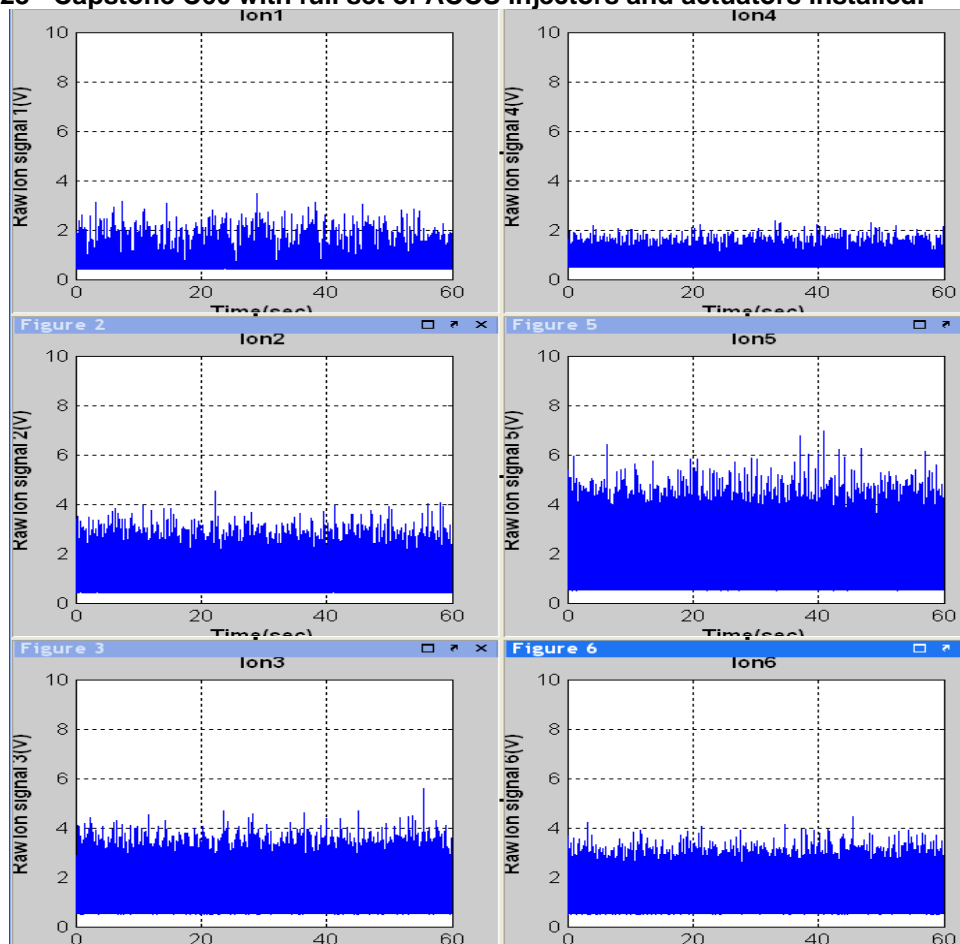


Figure 29 - Raw Ion Signal vs Time (sec) - Six Injectors.

3.2.3 Correlation Development

In an effort to develop a generalized correlation between the ion signal and pollutant emissions, a statistically designed experiment was developed. This systematic testing was intended to lead to the transfer function between ion signal and emissions that will be programmed into the engine control system. The first test matrix was a two-level factorial consisting of four factors: load, CO₂ dilution, turbine exit temperature, and actuator angle. There were four measured responses included in the matrix, NO_x and CO concentration in the exhaust stream, average ion signal voltage and the %DC of the ion signal. The ranges of the factors and the test matrix are shown in Table 1.

Table 1 - Initial Two Level Factorial Design with Repeated Centerpoint.

Std	Run	Factors				Responses			
		Load % max	%CO ₂	TET, degC	Actuator Angle, deg	NO _x	CO	Avg Ion	%DC
9	1	50	0	1115	12				
11	2	50	25	1115	12				
6	3	100	0	1175	0				
2	4	100	0	1115	0				
3	5	50	25	1115	0				
17	6	75	12.5	1145	6				
5	7	50	0	1175	0				
15	8	50	25	1175	12				
14	9	100	0	1175	12				
7	10	50	25	1175	0				
12	11	100	25	1115	12				
1	12	50	0	1115	0				
4	13	100	25	1115	0				
19	14	75	12.5	1145	6				
13	15	50	0	1175	12				
10	16	100	0	1115	12				
8	17	100	25	1175	0				
18	18	75	12.5	1145	6				
16	19	100	25	1175	12				

Initial testing revealed several flaws in the design of this matrix. The Capstone C60 uses injector staging for partial load demand. At both 75% and 50% load, at least one injector was not fired. This skewed the emissions results for the run as well as skewing the ion signal from the unfired injector. It was also determined that three of the factors (load, turbine exit temperature and actuator angle) were all, fundamentally, changing the equivalence ratio of the injector. In order to make the data more useful and consistent, it was decided that turbine exit temperature was an unnecessary factor to vary and only complicated the analysis. Though load and actuator angle both affect the equivalence ratio, it was deemed important to analyze the effect of both since the actuator angle changes the airflow through the injector, while load does not.

Another issue seen during the initial run of the test matrix was the variation in the emissions measurements. The repeated centerpoint tests showed variation of NO_x emissions spanning 43% of the total NO_x variation. This occurred because the data value recorded for the emissions came from a single “instantaneous” reading of the

emissions monitor at a specific time during the 60 second data collection period rather than an average of points. As a result, the emissions measurements were based on readings averaged over the same 60 second period as the ion signal recording.

During testing several of the ACCS injectors stopped generating an ion signal. Upon removal from the engine it was discovered that the ion probes had melted down to the point of fuel injection. Examples of the damage can be seen in Figure 30. The data showed that the ion signal stopped after the first run with the actuator angle set to 12°. Testing in the atmospheric injector rig showed that, with the actuator at 12°, the tip of the ion probe began to glow (Figure 31). It is believed that, as the tip of the probe began to glow, it provided an ignition source for the incoming fuel and air mixture. As the probe began to oxidize and melt, it pulled the flame back into the injector body, eventually grounding the ion probe and causing a lack of signal. It is important to note that the engine continued to run despite the damage to the injectors. In order to preserve the ion probes and decrease the likelihood of repeating the problem, the range of actuator angle was reduced from 0-12° to 0-9°. The reduction in angle range could potentially lead to a limit on the minimum NO_x achieved (recall Figure 5). However, maintaining integrity of the hardware is vital.

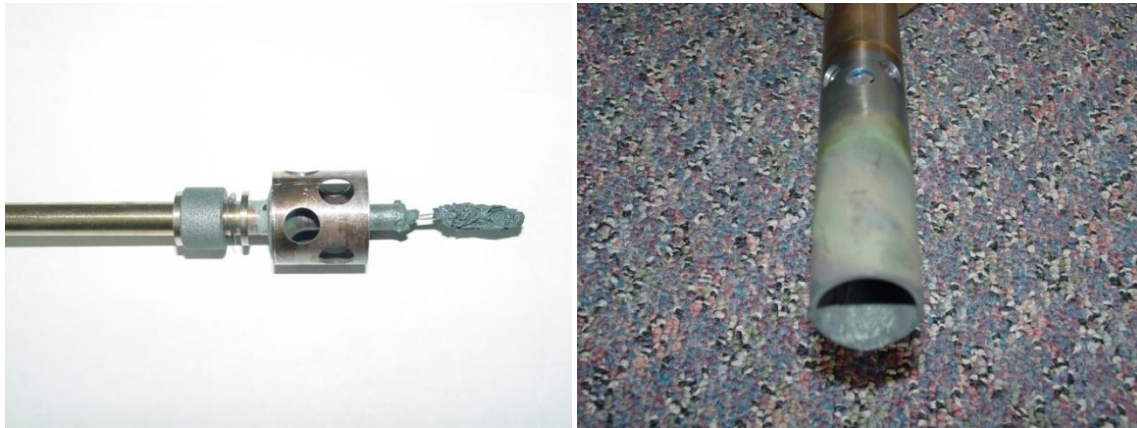


Figure 30 - Damaged center assembly and outer tube of injector.

Additionally, the range of load tested was decreased in order to ensure that all six injectors remained operational during the entire test. It was also suggested by Woodward that the standard deviation of the ion signal could be of value in developing the control algorithm. As such it was added to the revised test matrix shown in Table 2.

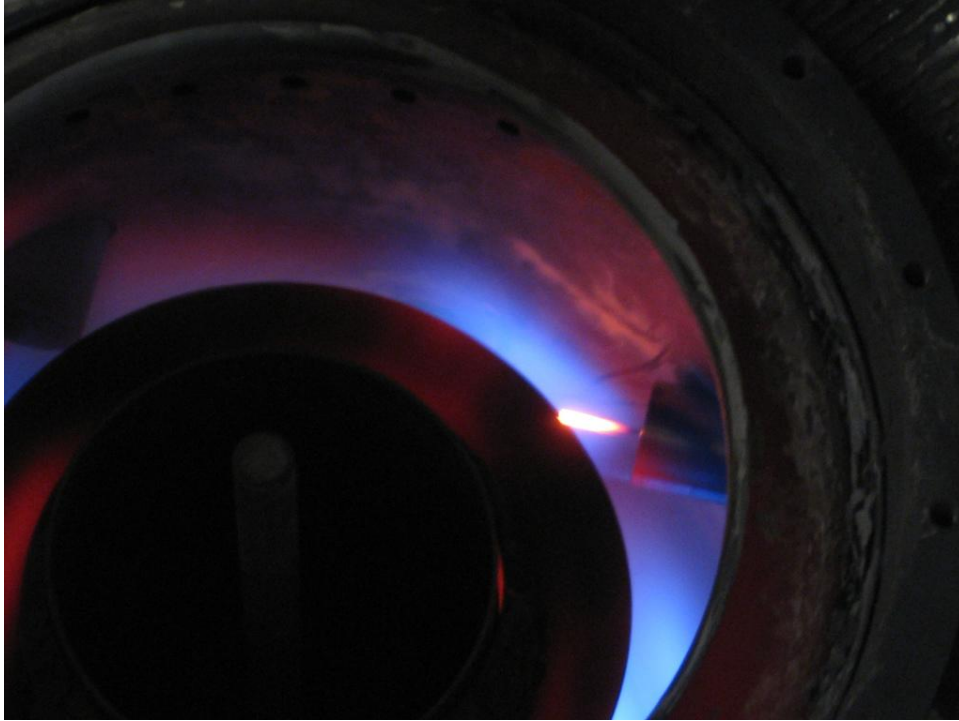


Figure 31 - Ion probe glowing due to actuator angle.

Table 2 - Revised Two Level Factorial Design with repeated centerpoint.

Std	Run	Factors			Responses			
		Load % max	%CO ₂	Actuator Angle, deg	NOx	CO	Avg Ion	%DC
9	1	80	0	9				
13	2	80	25	9				
7	3	100	25	0				
10	4	80	0	9				
8	5	100	25	0				
12	6	100	0	9				
14	7	80	25	9				
2	8	80	0	0				
16	9	100	25	9				
5	10	80	25	0				
17	11	90	12.5	4.5				
11	12	100	0	9				
19	13	90	12.5	4.5				
15	14	100	25	9				
4	15	100	0	0				
6	16	80	25	0				
3	17	100	0	0				
1	18	80	0	0				
18	19	90	12.5	4.5				

Analysis of variance of the measured values did not indicate any statistical relationship between the responses and the factors varied. The reason for this is associated with the high level of variability in the signals. The ion signal showed significant variation between injectors, as well as variance from the same injector on different days. This was despite great care being taken to ensure that all of the probes had the same length of extension to within an estimated ± 0.3 mm tolerance. As shown in Figure 32, the range of the ion signal also varied greatly between the tests. Injector 1 shows a total variation of less than 0.2 V, while injector 2, on the same plane, shows a variation of nearly 1.0 V. This discrepancy in range across multiple loads is also apparent in the aft plane injectors.

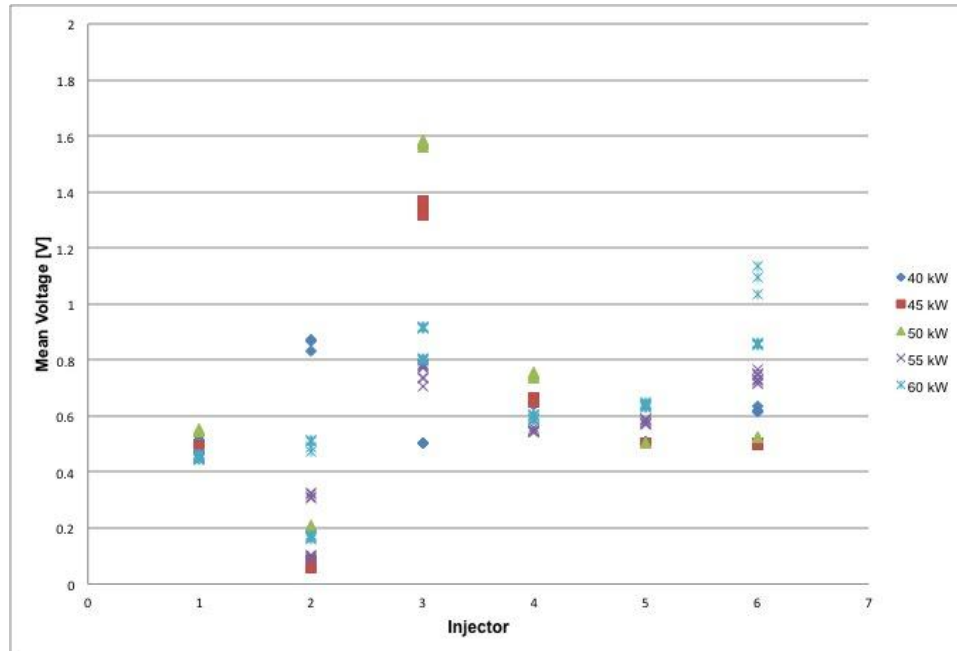


Figure 32 - Ion Signal Variation.

Perhaps more indicative of the issue is the range of standard deviation for the same set of tests. As shown in Figure 33, the standard deviation is on the same order of magnitude as the average ion signal voltage. Additionally, the range of standard deviation varies significantly between injectors. There also does not appear to be a significant trend between the load and the standard deviation. For instance, the 55 kW case, a condition in which all six injectors are fired, has the lowest standard deviation on injectors one through four, yet is near the highest on injectors five and six.

As a result of these investigations, it became apparent that while individual runs demonstrated reasonable correlations with various aspects of the ion signal, the overall repeatability and robustness of the current strategy remains a question. This is attributed to the adoption of the centerline probe location which was subject to thermal growth and distortion which likely was a function of stop/start cycles, load variations and even actuator positioning. Hence while the ion sensing approach offered a number of promising attributes, the observed lack of robustness indicates additional considerations regarding the specific implementation for the engine used in this study.

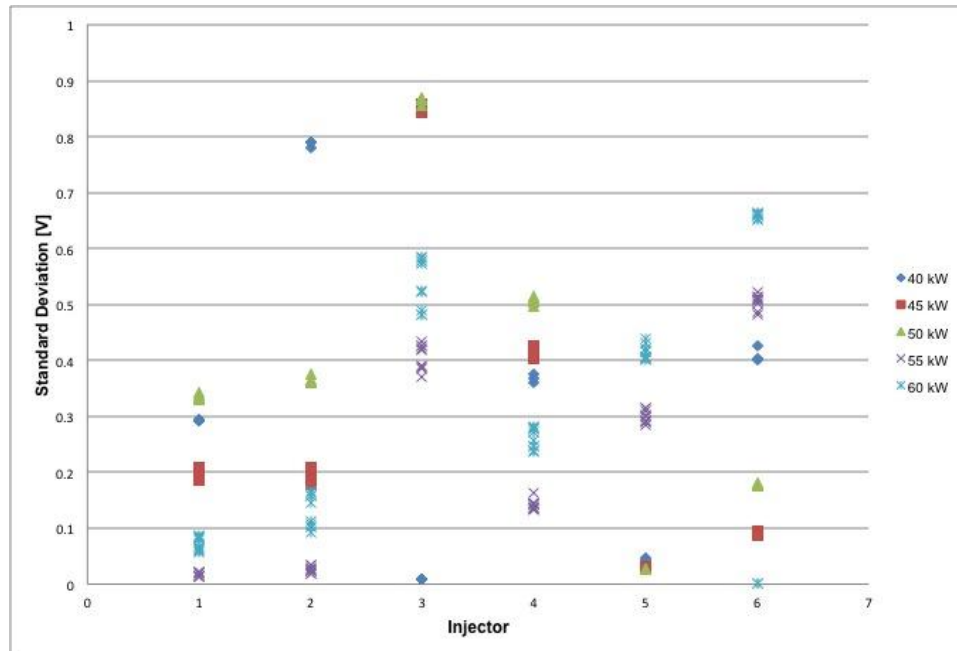


Figure 33 - Variation of Standard Deviation.

3.3 Algorithm Integration

Extensive discussions were held between Capstone, Woodward, and UCI regarding the best approach for integration of the control system. The ultimate integration would involve the programming of the sensor/emissions/actuation signals into the Capstone control system. Examination of the Capstone firmware and software indicates that this is straightforward, but time consuming. Prior to committing to this step, it was deemed to be in the best interest of the parties to do testing using separate systems—one for engine control, and one for injector control. The logic of this arrangement is reasonable and no conflicts are apparent between the two systems. Some signals from the Capstone data recording system can be easily passed to the Woodward system. Such signals are needed to minimize any problems with hardware damage. However, this is not needed for the prototype demonstration planned. Furthermore, the inability of the algorithm development step to produce a definitive relationship between ion signal and emissions essentially precluded this step to be taken in subsequent tests.

3.4 Field Test

Although some shortcomings were evident with the incorporation of ion sensing into the C60 injectors, some major improvements in actuation and sealing were accomplished and demonstrated in the engine tests carried out at UC Irvine. As a result, it was worth evaluating the robustness of these elements in the field. In addition, emissions testing could be carried out for different actuator settings to demonstrate that the injector control approach could indeed affect emissions as originally intended.

The original field test site was the Calabasas landfill operated by the LA County Sanitation Districts. This site was attractive because (1) it had 30 kW MTGs operating

on landfill gas and (2) it had appropriate gas clean up and pressurization required to operate the current MTG. As a result, to incorporate the current engine, it could either be added to existing “train” of MTGs on site or it could be used to effectively replace two of the existing 30 kW units. Unfortunately, due to timing of the current project and ongoing efforts at the landfill, the opportunity to utilize the site passed. The MTG installation was effectively retired and revamped to incorporate a 5MW Solar Mercury 50 gas turbine.

As a result, UC Irvine worked with some alternative candidates, including Bowerman landfill in Irvine as well as waste water treatment plants at Eastern Municipal Water District (EMWD) and Santa Margarita Water District (SMWD). After evaluation of the options and meeting with the candidate sites, UCI ended up working with Ron Meyer at the SMWD. A site at the Chiquita Water Reclamation Plant was evaluated for suitability and it was concluded it could work well. The CWRP already had four 30 kW MTGs operating on site and had water flow capacity to fire additional MTGs. Some time was taken to arrive at an appropriate Memorandum of Understanding between UC Irvine and SMWD and once in place, efforts were undertaken by both sides to arrange for delivery and installation of the unit.

Because of use of a waste water treatment facility, the variation in actual gas composition was not expected to be very large. The facility processes 9 MGD of wastewater and produces 105,000 ft³/day of digester gas. The typical methane content is 55-60%. A landfill derived biogas composition can vary more substantially which is the reason the original site pursued was a landfill.

SMWD poured an additional slab portion to accommodate siting the unit. In addition, they set up a circuit breaker box to tie the MTG into and established a gas hookup point. UC Irvine delivered the MTG to the site on 30 June 2011. At this point, the plan included installation of metering equipment to allow monitoring of the engine performance. A few additional visits were required to detail the requirements to physically connect the engine to the breaker box and gas hookup point. Figure 34 shows the positioning of the MTG along with the general equipment at the site.

- a) Dropping MTG onto newly poured slab.



- b) MTG adjacent to existing 30 kW units and Micogen heat recovery unit.



Figure 34 - Installation at Santa Margarita Water District Chiquita Water Reclamation Facility.

On 28 July, 2011, the engine hookup was completed and the engine was started up with injectors positioned at nominally “optimum” conditions for the gas composition at CWRP (~60% methane). The engine ran until 7 August 2011 at which time an electrical trip

occurred. UCI personnel visited the site 8 August 2011 and it was concluded that a fuse in the breaker box had blown—hence the fault was not associated with the engine itself. The fuse was replaced the engine started again. The engine was running continuously up to the time of this report (through December 2011) with at least 3,700 hours of operation. The operation of the engine during this time was >99%.

In parallel with the unit demonstrating satisfactory operation, plans for metering equipment were finalized to monitor performance. The metering equipment installation plan was developed and approved by the demonstration site personnel and this equipment was procured and assembled at UCI. The collection of metering equipment was incorporated into the installation by UC Irvine personnel on 28 October 2011. Electric power was monitored via a Dent Elite Power meter with voltage taps and current transformers installed on the three phase leg outputs. The Dent Meter logs a number of user defined parameters (phase voltage, current, overall power, power factor, etc) at a user defined intervals. The gas flow was measured with a Sage insertion thermal mass flow meter. To insure properly conditioned flow in the 1-1/2" pipe presented to the flow meter, a 36-inch length of straight pipe upstream and 12 inches downstream was installed on the gas line upstream of the MTG. The Sage meter measures a value of flow rate once calibrated with the thermal properties of the gas and provides with a 4-20 mA output signal that was recorded by a separate Dent Data Logger Pro. Ambient temperature and relative humidity were recorded with a separate, ACR brand data logger. All loggers were synchronized in time and recorded average values over a 10 minute window for a period that extended to January 1, 2012. Figure 35 shows the plumbing needed to incorporate the gas flow meter into the circuit.

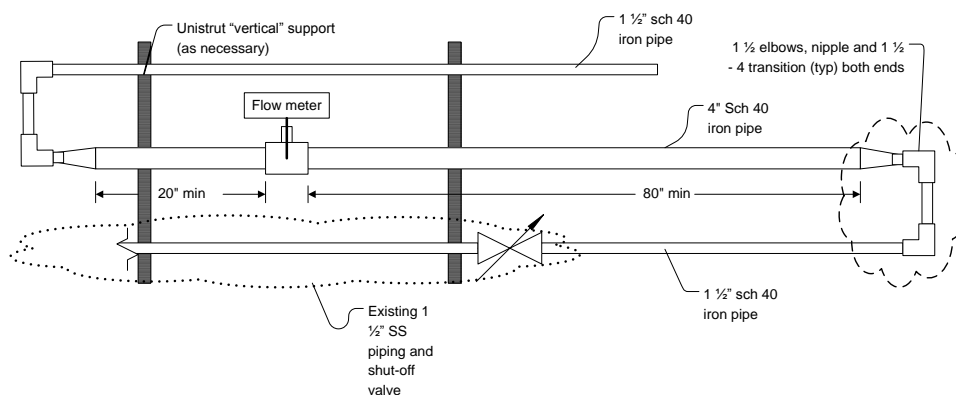


Figure 35 - General Layout of Plumbing to Incorporate Gas Flow Metering.

Using the installed metering equipment, gas flows and electrical output was logged continuously for 22 days. The gas metering sensor failed at this point and thus efficiency information is provided only on these 22 days of operation. The results are shown in Figure 36. The average fuel to electricity efficiency is 24% (based on Higher Heating Value). The average output during the period was 45 kW. The drops in output and efficiency are seemingly associated with limited digester production during cold periods. Despite being “starved” for fuel, the engine continued to run. Average temperatures in early November were at or below normal, whereas from 9 November onward the ranges were within normal (see Figure 37). Electrical output readings continued through 1 January 2012 and are shown as well on Figure 36. Note that on 15 November 2011, the output requested from the engine was reduced to 50 kW. This was done because the added fuel consumption for the demonstration engine was taxing the

output of the anaerobic digester which was impacting operation of all the engines on site. As a result, the power output setting was reduced to 50 kW to allow all the engines on site to run more smoothly with minimal fuel starvation. The strategy was successful as indicated by the relatively constant output at 50 kW from 15 Nov 2011 and later. Some period are noted where the engine outputs minimal power. These were periods where maintenance was being done which reduced or stopped the fuel flow.

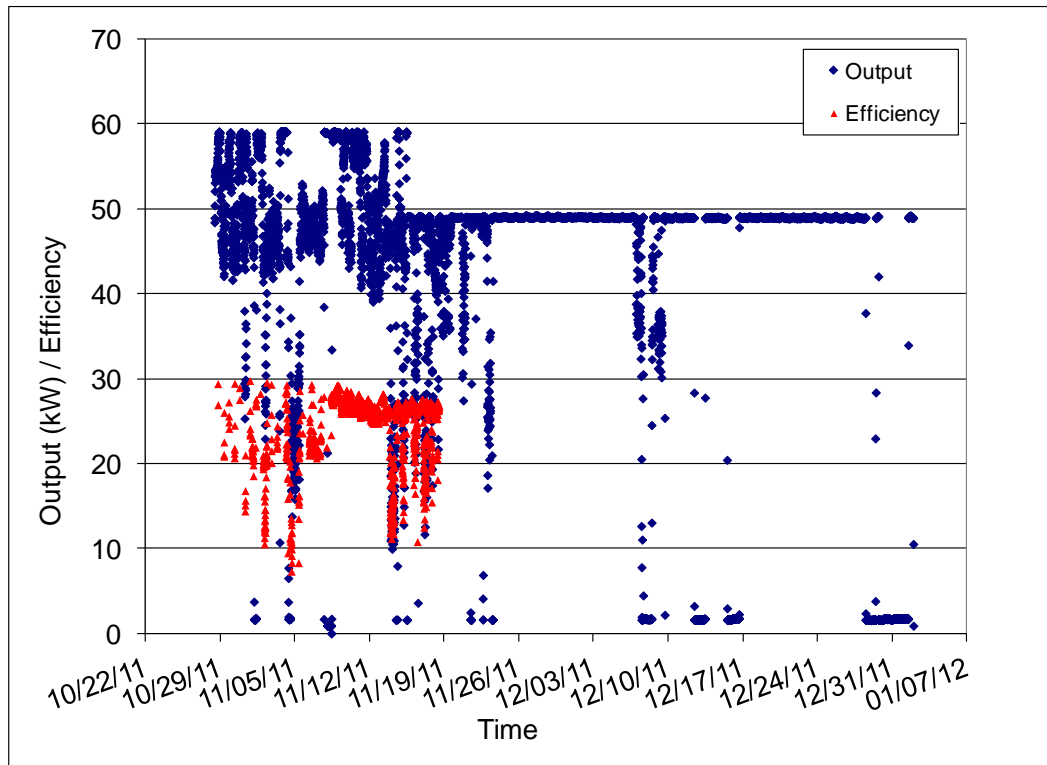


Figure 36 - Output and Efficiency 28 Oct to 1 Jan 2012.

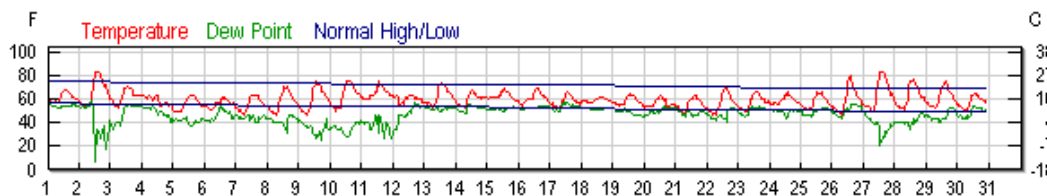


Figure 37 - Temperatures in November 2011.

Finally, emissions measurements were obtained in the field. These results are summarized in Table 3. For emissions, two cases were considered. In the first case, three of the injector actuators were moved away from nominal position. As shown, moving these injectors away from optimal position resulted in changes in emissions, in particular NO_x. The optimized position results bring the NO_x levels back to expected low levels, confirming sensitivity to the actuator position observed in the laboratory tests could be reproduced in the field. The other important point about this test is that smooth injector actuation could be attained even after 3,700 hours of operation indicating robustness of the Woodward design.

Table 3 - Field Emissions Levels.

Injector State	Species				
	O ₂ , %	CO ₂ , %	CO ^{/1} , ppmvd	NO ^{/1} , ppmvd	NO _x ^{/1} , ppmvd
Non-optimized	17.1	2.99	9.7	11.9	16.5
Optimized	17.1	2.96	26.4	0.9	3.4

^{/1} Corrected to 15% O₂.

In summary, the field test, while not able to test a fully closed-loop control system, was able to confirm several important steps. First, the advanced sealing and improved actuation strategies incorporated with the expertise of Woodward were fully successful in preventing leaks and faulty motion that were major issues at the outset of this project. Second, it was shown that the actuated injectors can affect emissions in the field. As a result, it is expected that with a suitable sensing system, the general approach is viable.

4 Status of the Technology

As of the close of this study, this technology is ready for the next step toward commercialization. The project evaluated ion sensing as an alternative to the previously studies optical method as a sensor for an active combustion control system that will allow the cost targets to be met. The project also addressed major weaknesses in the initial prototype systems including thermal management issues, sealing, and actuation. It also demonstrated that general trends could be found to correlation the ion signal with both NO_x and CO. However, the specific implementation used in the current effort suffered from a high level of variability due to the high sensitivity of the signal to ion probe positioning as a result of several factors, including thermal growth, installation procedures, and wear. Despite this, the Capstone C60 microturbine was demonstrated for >3000 hours with the ion sensing injectors installed and the major weaknesses identified in the previous project were clearly addressed with the new design.

In order to be considered completely commercially ready, additional steps for future work on the adaptive low emission microturbine generator include:

- An alternative ion sensing implementation for the C60 injectors needs to be established to reduce the sensitivity of the signal to allow specific robust correlations to be developed. Since the length of the ion probe is a critical dimension, a system with less adjustability would be preferable. It is possible an optical method could provide the robustness needed, but would likely cost more to implement. Using lower cost components such as avalanche photodiodes could result in added cost of less than \$150/kW to monitor all 6 injectors compared to the \$50/kW target realized by the ion sensing technology.
- The installation process for the injectors could be made easier and more accurate if the injectors were produced with an index mark and way to lock the injectors in the fully open position.
- Currently, the injectors and actuators protrude beyond the case of the engine, necessitating the running of the engine without the noise-reducing side panels. For a system in the field, this would not be acceptable in some settings.

- The ACCS system should be at least partially integrated into the Capstone engine control system for most reliable operation. This could be pursued once a robust sensor strategy is identified.
- Beyond the C60 consideration, application of ion sensing to a combustor with a configuration more amenable to this method should be pursued. For example, implementation on combustion systems with fuel injectors with annular passages around a centrally located flameholder has already proven successful.¹³
- In additional field testing, it would be of great interest to document emissions while changing from the biogas to natural gas. This could be necessary if conditions at the plant led to a reduction in digester gas flow and had a means to co-fire natural gas (the current site does not have this capability). This would represent the extreme condition in fuel compositional change that this technology could potentially address from an emissions impact standpoint.

5 References

¹ Simons, G. and Zhang, J. (2001). "Distributed Generation from Biogas in California", Presented at Interconnecting Distributed Generation Conference, Mar 21.

² Lemar, P. (2004). Opportunity Fuels for CHP: Alternative to High Gas Prices?, Presented at the 5th Annual CHP Roadmap Workshop, Austin Texas, Sept 22.

³ Phi, V.M., Mauzey, J.L., McDonell, V.G., and Samuelsen, G.S. (2004). Fuel injection and emissions characteristics of a commercial microturbine generator, Paper GT-2004-54039, TurboExpo 2004, Vienna, Austria.

⁴ McDonell, V.G., Effinger, M.W., and Mauzey, J.L. (2006). Correlation of Landfill and Digester Gas Composition with Gas Turbine Pollutant Emissions, Paper GT2006-90727, Presented at ASME Turbo EXPO 2006, Barcelona, Spain, May.

⁵ Tillman, D.A. and Harding (2004). Fuels of Opportunity: Characteristics and Uses in Combustion Systems, Elsevier, Oxford, UK.

⁶ Docquier, N. and S. Candel (2002). Combustion control and sensors: a review. *Progress in Energy and Combustion Science* **28** (2): 107-150.

⁷ Ballester, J. and Garia-Armingol (2010). Diagnostic techniques for the monitoring and control of practical flames, *Progress in Energy and Combustion Science*, Vol. 36, pp. 375-411.

⁸ Bandaru, R. V., S. Miller, J.-G. Lee and D. A. Santavicca (1999). Sensors for measuring primary zone equivalence ratio in gas turbine combustors. Advanced Sensors and Monitors for Process Industries and the Environment, Boston, MA, USA, SPIE.

⁹ Ballester, J., Hernandez, R., Sanz, A., and Barroso, J. (2009). "Chemiluminescence monitoring in premixed flames of natural gas and its blends with hydrogen," *Proceedings of the Combustion Institute*, Vol. 32(2), pp. 2983-2991.

¹⁰ Demayo, T.N., McDonell, V.G., and Samuelsen, G.S. (2002). Robust Active Control of Combustion Stability And Emissions Performance In A Fuel-Staged Natural Gas-Fired Industrial Burner. *Twenty-Ninth Symposium (International) on Combustion*, The Combustion Institute, pp. 131-138.

¹¹ Muruganandam, T.M., Nair, S., Scarborough, D. Neumeier, Y., Jagoda, J, Lieuwen, T., Seitzmann, J., and Zinn, B.T. (2005). Active control of lean blowoff for turbine engine combustors, *J. Propulsion and Power*, Vol., 21(5), pp. 807-814,

¹² Thornton, J. (2006). Private Communication.

¹³ Benson, K., Thornton, J. D., Straub, D. L., Huckaby, E. D., Richards, G. A.(2003), "Flame ionization sensor integrated into gas turbine fuel nozzle," GT2003-38470, Proceedings of Turbo Expo 2003, June 16-19, Atlanta, GA.

¹⁴ McDonell, V.G., Mauzey, J.L., and Samuelsen, G.S., "Low NO_x—Low CO MTG Combustor" (2006), California Energy Commission Final Report (Draft), Contract 500-00-020, Project 3, Feb 2006.

¹⁵ Leonard, G. and Stegmaier, J. (1994). Development of an Aerodervative Gas Turbine Dry Low Emissions Combustion System, *J. Engr for Gas Turbines and Power*, Vol. 116, pp. 542-546.